Detailed Anatomical and Functional Features of the Cardiac Valves

7

Michael G. Bateman, Jason L. Quill, Alexander J. Hill, and Paul A. Iaizzo

Abstract

The use of high-resolution noninvasive imaging in modern cardiac clinics to collect detailed images of valve function has dramatically accelerated the understanding of functional human heart anatomy. In the healthy human, the cardiac valves determine the passage of blood through the heart. The atrioventricular valves open during diastole to allow the filling of the ventricles and close during systole (ventricular contraction), directing blood through the semilunar valves to the body; these valves, in turn, close during diastole to prevent the flow of blood back into the ventricle. By presenting a comprehensive review of the histology, functional anatomy, and morphology of the cardiac valves, this chapter promotes an understanding of the valve features that is required for valvar repair or replacement via either surgical or minimally invasive (transcatheter) means.

Keywords

Atrioventricular valve • Semilunar valve • Mitral valve • Tricuspid valve • Aortic valve • Pulmonary valve • Imaging

Abbreviations

APM	Anterior papillary muscle complex (superoposterior)
PPM	Posterior papillary muscle complex (inferoanterior)

7.1 Introduction

A critical understanding of cardiac anatomy is essential for design engineers and clinicians with the intent of developing and/or employing improved or novel technologies or therapies for treating an impaired cardiac valve. Likewise, such knowledge is required for directing translational research, including initiating preclinical investigations, assessing the feasibility of clinical trials, and performing first-in-man procedures. There are two atrioventricular valves in the human heart, namely, the *tricuspid and mitral valves*. Likewise, there are two arterial valves in the human heart, specifically the *pulmonary and aortic valves.* All valves are complex structures whose normal anatomical structure can vary greatly among individuals and/or also become modified by disease processes. In this review, we discuss the anatomy, pathology, and issues related to transcatheter and surgical repairs of the atrioventricular and arterial valves in a translational manner.

The high prevalence of aortic valvar pathologies in the burgeoning elderly population, coupled with poor clinical outcomes for patients who go untreated, has resulted in prolific spending in the research and development of more effective and less traumatic therapies. The accelerated development of therapies designed to treat the arterial valves has been guided by anatomical information gathered from high-resolution imaging technologies, which in turn have focused attention on the need for complete understanding of arterial valvar clinical anatomies.

M.G. Bateman, PhD (✉) • J.L. Quill, PhD • A.J. Hill, PhD
Medtronic, Inc., 8200 Coral Sea St. NE, Mounds View, Minneapolis, MN 55112, USA
e-mail: michael.g.bateman@medtronic.com

P.A. Iaizzo, PhD
Department of Surgery, University of Minnesota, Minneapolis, MN 55455, USA

P.A. Iaizzo (ed.), *Handbook of Cardiac Anatomy, Physiology, and Devices*, DOI 10.1007/978-3-319-19464-6_7

7.2 The Cardiac Skeleton

Before describing the specific anatomies of the cardiac valves, it is important to understand the anatomical framework that holds these valves in position and thus consequently the relationships of each valve to one another [1]. Figure 7.1 shows an anatomical plate of a human heart with the atria and great arteries removed, highlighting the close proximity of all four cardiac valves to each other. Traditionally, the four valves of the heart have been described as being supported by a fibrous framework or *cardiac skeleton* made of dense connective tissue passing transversely through the base of the heart between the atria and the ventricles. As described by Wilcox, Cooke, and Anderson [1] and by Bateman et al. [2], the strongest part of the skeleton is the area of fibrous continuity between the leaflets of the mitral and aortic valves. This fibrous strap, thickened at both its ends by the fibrous trigones, anchors the aortic-mitral valvar unit within the base of the left ventricle (Fig. 7.2). The coronet-like support of the aortic valvar leaflets extends antero-cranially from the region of fibrous continuity and is often considered to represent an aortic valvar annulus, but there are no anatomical structures supporting the semilunar hinges of the aortic valvar leaflets (Fig. 7.3) [2]. The right fibrous trigone is itself continuous with the membranous part of the ventricular septum and is an integral part of the aortic coronet (Fig. 7.2). The trigone and membranous septum together are usually described as the central fibrous body. The smaller left fibrous trigone is formed at the leftward end of this zone of fibrous continuity [4]. Inconstant cords of fibrous tissue then extend from the margins of the fibrous continuity between the aortic and mitral valve to support the mural (anterior) leaflet of the mitral valve.

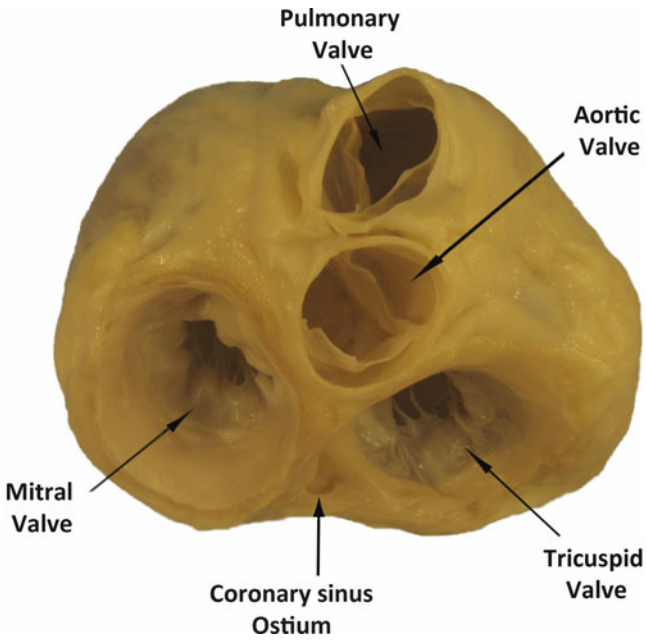

Fig. 7.1 An anatomical plate of a human heart with the atria and great arteries removed showing the relationship between the four valves at the base of the heart. Note the fibrous connection between the leaflets of the mitral valve creating a double orifice valve

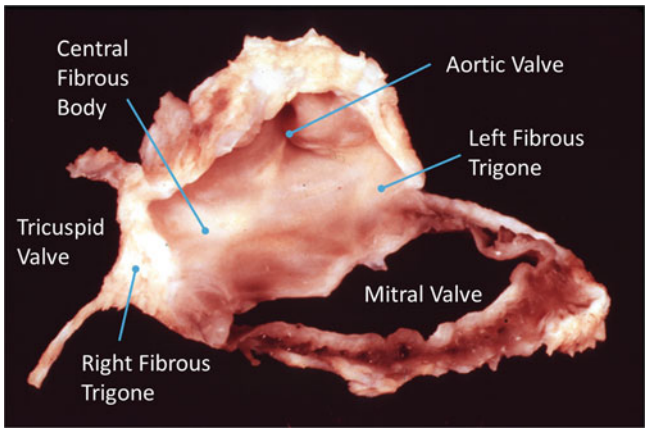

Fig. 7.2 Dissection of the cardiac skeleton showing the aortic valve (*center*), the mitral valve annulus (*below right*), and the fibrous sections of the tricuspid valve (to the *left*). The original image for this figure was kindly provided by Professor Robert H. Anderson. It was initially published in "Cardiac Anatomy" [3] and has been modified for this review. Professor Anderson retains the copyright of the initial image

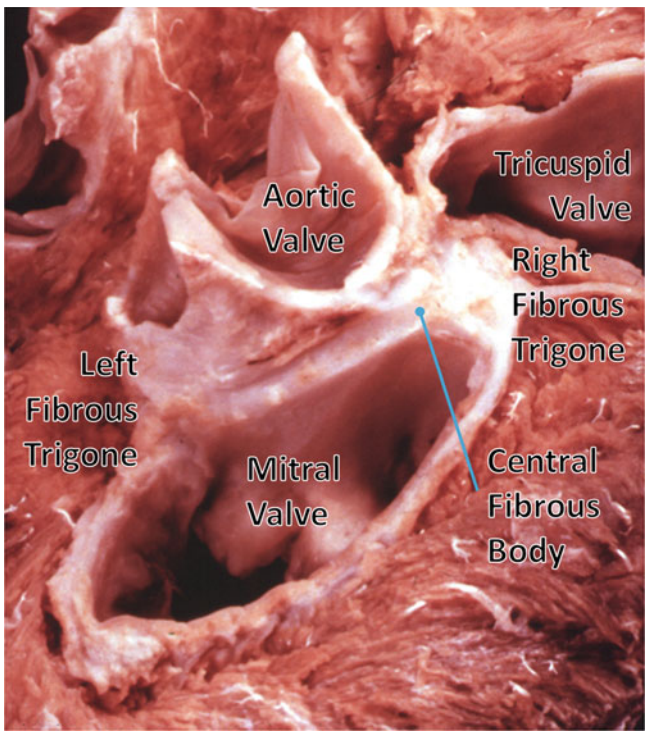

Fig. 7.3 Dissection of the cardiac skeleton with the atria and great vessels removed showing the coronet shape of the aortic annulus and the mitral valve. The original image for this figure was kindly provided by Professor Robert H. Anderson. It was initially published in "Cardiac Anatomy" [3] and has been modified for this review. Professor Anderson retains the copyright of the initial image

However, the extent of the skeleton is often greatly exaggerated. The so-called annular components of the atrioventricular valves then extend inferiorly and posteriorly from the central fibrous body and the left fibrous trigone, respectively (Fig. 7.3) [2]. It is the exception rather than the rule, however, for these fibrous cords to extend throughout the full circumference of the left and right atrioventricular junctions. The annuluses of the atrioventricular valves, as such, are better formed in the mitral as opposed to the tricuspid junction. In the mitral junction, it is normal to find segments of the valvar leaflets hinged from the fibroadipose tissue of the atrioventricular junction, rather than from a firm fibrous annulus [5]. In the tricuspid junction, the valvar leaflets are normally hinged from fibroadipose tissue [6]. The annuluses, as part of the atrioventricular junctions and rarely being complete fibrous rings, are highly dynamic and change dramatically in shape and size throughout the cardiac cycle from systole to diastole [1, 2]. It is also the fibroadipose tissue of the junctions that provides the greatest part of the insulation between the atrial and ventricular muscular masses, with the atrioventricular bundle of the conduction system being the only structure in the normal heart that crosses the insulating plane. The bundle penetrates through the atrioventricular component of the membranous septum.

The leaflets of the pulmonary valve have no direct fibrous support other than that provided by the valvar sinuses. The basal components of each leaflet are supported by the right ventricular infundibulum. It is this unique positioning of the pulmonary root away from the other valvar structures that makes possible its surgical removal during the Ross procedure, while the presence of the supporting skirt of infundibular musculature facilitates its use as an autograft to replace the aortic valve [7].

7.3 The Atrioventricular Valves

In the most basic anatomical sense, the atrioventricular valves are made up of three main components:

- Valve leaflets attached to the respective annulus
- Tendinous cords attaching the leaflets to the ventricular myocardium
- Papillary muscles providing the anchoring points for the tendinous cords to the ventricular wall

The leaflets of the atrioventricular valves can be thought as forming a *skirt* that hangs from the annulus; leaflets are divided into a series of sections that constitute the distinct leaflets of each valve. Due to the extent of variations between individuals with regard to leaflet morphologies, there has been much debate relative to nomenclature on the number of leaflets of both the mitral and tricuspid valves [8–10]. Traditionally, the division of the leaflets has been determined by the presence of commissures which can be described as the peripheral attachment of a break in the skirt [1].

The leaflets themselves are attached to the ventricles via the sub-valvar apparatus of each valve. In general, each apparatus consists of the tendinous cords and the papillary muscle complexes of each valve. The tendinous cords are usually categorized by (1) those that support the free edges of the valves, (2) those that support the rough zones (the region between the free edge and each annulus), and/or (3) those that attach to the leaflets near to the annulus. Typically, the cords supporting the free edges of the leaflets are known as *fan cords* due to the presence of multiple fenestrations. Those that attach to the rough zone of the leaflets are distinguished by their larger size and are commonly defined as *strut cords*. Finally, those that attach near the annulus are known as *basal cords*. The strut cords are of specific importance, as they bear the highest mechanical loads during systole [11]. Furthermore, the number and distribution of the tendinous cords across a given valve are critical to its function; it is well documented that dysfunction of these structures can lead to prolapse of the valves [12–14]. In general, the cords attach to the heads of the papillary muscles, which themselves play an important role in the function of each valve by contracting during systole to cushion the valve closure and help prevent the valve from prolapsing into the atrium.

7.3.1 Atrioventricular Valve Function

During systole, when the ventricles are contracting, the subvalvar apparatus of each valve prevents the leaflets from prolapsing into the atria and additionally aids in ventricular ejection by effectively drawing the apex of the ventricle toward the basal ring. Additionally, it has also been shown that the sub-valvar apparatus plays a crucial role during diastole, while the ventricle is filling, by moderating wall tensions and improving the efficiency of the ventricular myocardium [15, 16]. During systole in normal/healthy cardiac function, the valve leaflets, which bulge toward the atrium, can be considered to stay pressed together throughout the contraction and therefore do not prolapse. During diastole, when the ventricles are relaxing and the chambers are filling through the open atrioventricular valves, eddy currents that form behind the leaflets and tension in the subvalvar apparatus keep the leaflets close together.

Figures 7.4 and 7.5 show image sequences obtained employing Visible Heart® methodologies, as described in Chap. 41. These sequences display the normal cardiac function of the mitral and tricuspid valves, respectively [17, 18]; the images were obtained from the atria (above the valve) and from the ventricular apexes (below the valve).

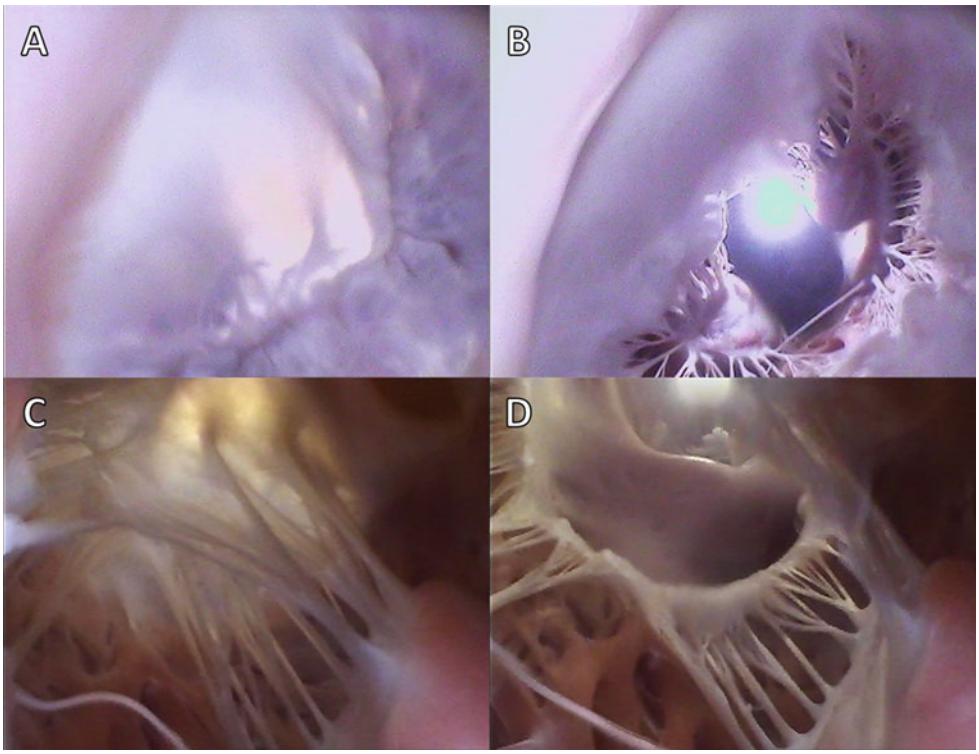

Fig. 7.4 Internal videoscopic images of the mitral valve from above (**a**, **b**) and below (**c**, **d**) during systole (**a**, **c**) and diastole (**b**, **d**) obtained employing Visible Heart® methodologies

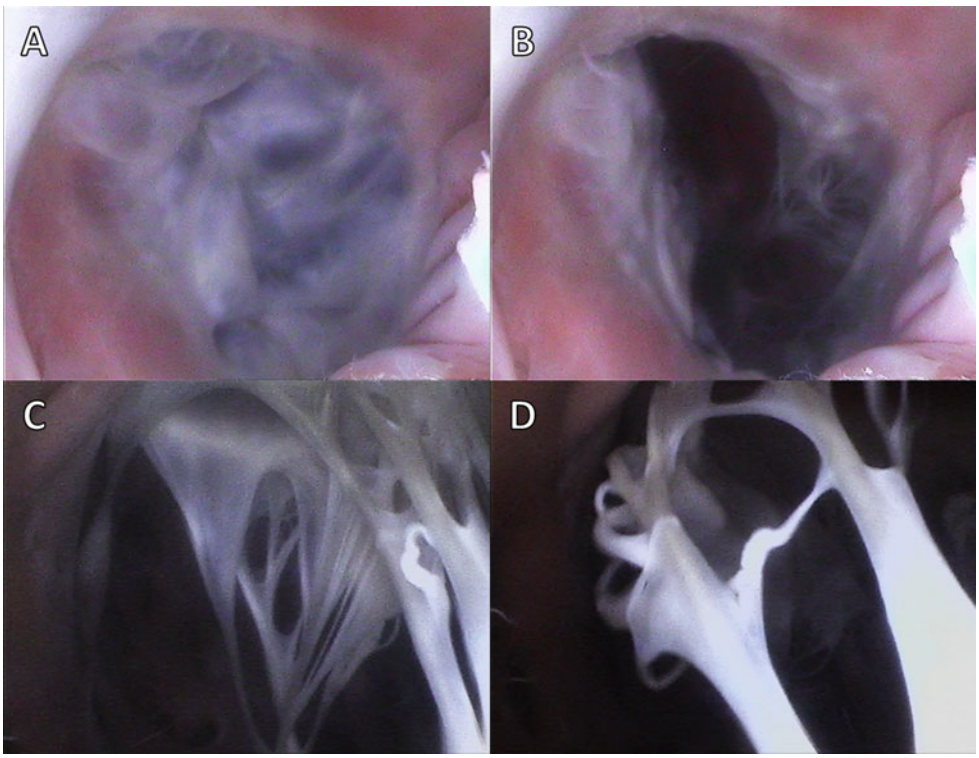

Fig. 7.5 Internal videoscopic images of the tricuspid valve from above (**a**, **b**) and below (**c**, **d**) during systole (**a**, **c**) and diastole (**b**, **d**) obtained employing Visible Heart® methodologies

Dysfunction of the atrioventricular valves is usually characterized by one of two symptoms: (1) failure of a valve to successfully close or (2) failure of a valve to successfully open. Dysfunction of the valves during systole (i.e., failure of the valve to successfully close) is known as valvar *incompetence* and results in the *regurgitation* of blood back in a retrograde direction though the atrioventricular junction. Such dysfunction results in a decrease in cardiac output and also increases the pressure within the atria during systole (potentially causing atrial dilation and/or eventually atrial

fibrillation). Dysfunction of the valves in diastole (failure of the valve to fully open and allow blood to fill the expanding ventricles) is termed *stenosis*. This decrease in effective orifice area of the open valve is often due to stiffening or calcification of the valve leaflets.

7.4 The Semilunar Valves

A healthy semilunar valve is composed of three valve leaflets, each attached to its respective sinus. These valves lie between the ventricular outflow tracts and the arterial trunks, the main arteries carrying blood away from the heart. This elegant structure is much simpler than that of the atrioventricular valves described previously, in that the semilunar valve leaflets do not require a tension apparatus to maintain competency. When closed, the three leaflets of each valve coapt along zones of apposition, or *commissures,* which are fibrous zones some distance from the free edge of the leaflets. At the center of the valve where all three leaflets coapt, a distinct fibrous nodule can be found. The valve leaflet margins are attached to the arterial wall in the shape of a half-moon, hence the *semilunar* moniker. Normally, the regions of the valves where the commissures meet the arterial wall are considerably higher than the seats of the leaflets, thereby giving the valve a crown-like shape. These three points, particularly in the aortic valve, are used to define the sinotubular junctions (Fig. 7.6). Although we have discussed the positioning of the valves in the heart by referring to their respective annuluses, many anatomists contest the idea that there are single defined annuluses for both the pulmonary and aortic valves [19]. Interestingly, there is a defined annulus where the respective arteries are attached to the ventricular outflow tract; however, due to the crown-like structure of the valve, the hemodynamic junction of the valves spans this annulus. This structural shape results in part of the arterial wall being considered a ventricular structure (in a hemodynamic sense) and, in turn, part of the ventricular wall an arterial structure. Just distal to the valves are the *arterial sinuses* that are represented by dilations of the artery positioned above each leaflet and additionally house the coronary artery ostium. The sinus also provides a recess for the valve leaflets to retract into, allowing for unrestricted flow from the ventricle to the artery. Finally, the virtual ring, upon which many annular measurements are based and which defines the basal plane of aortic valve, is defined by the three anatomical anchors at the nadir of each aortic leaflet [20]. These features are illustrated by the diagram in Fig. 7.6. The position and definition of the valve annulus is often contested by different medical specialists, and a recent questionnaire highlighted the current lack of consensus between physicians regarding the optimal means of describing the semilunar valve anatomy [21]. As such, it is important to be precise in the definition of exactly what is being measured when documenting the size and shape of the semilunar valve annuluses.

7.4.1 The Functioning of the Semilunar Valves

When a semilunar valve is functioning correctly, the leaflets are pushed into the sinus during myocardial contraction (systole) to allow blood to leave the ventricles. As the myocardium relaxes and the pressure within the ventricle drops below the pressure distal to the valve in the arterial system (the aorta or pulmonary artery), the valve snaps shut. This usually happens soon after ventricular systole but before the heart has completely relaxed, so that during diastole, when the chambers are filling through the atrioventricular valves, the leaflets of the semilunar valves remain tightly closed. A positive pressure difference between the aorta and the coronary sinus, which lies within the right atrium, allows for the flow of blood through the coronary vasculature. Thus, it should be noted that the heart muscle is perfused with blood when the semilunar valves are closed and the cardiac myocytes are relaxing.

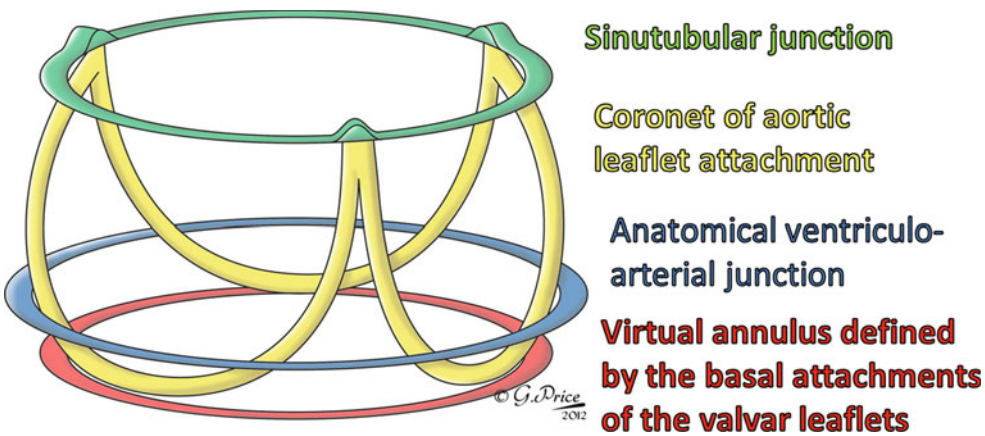

Fig. 7.6 Idealized three-dimensional arrangement of the semilunar valve (this diagram represents an aortic root). The model contains three circular rings with the leaflets suspended within the root in crown-like fashion. The cartoon is reproduced with kind permission of Professor Robert H. Anderson who retains the intellectual copyright in the original image. Special acknowledgment goes to Gemma Price as the artist [7]

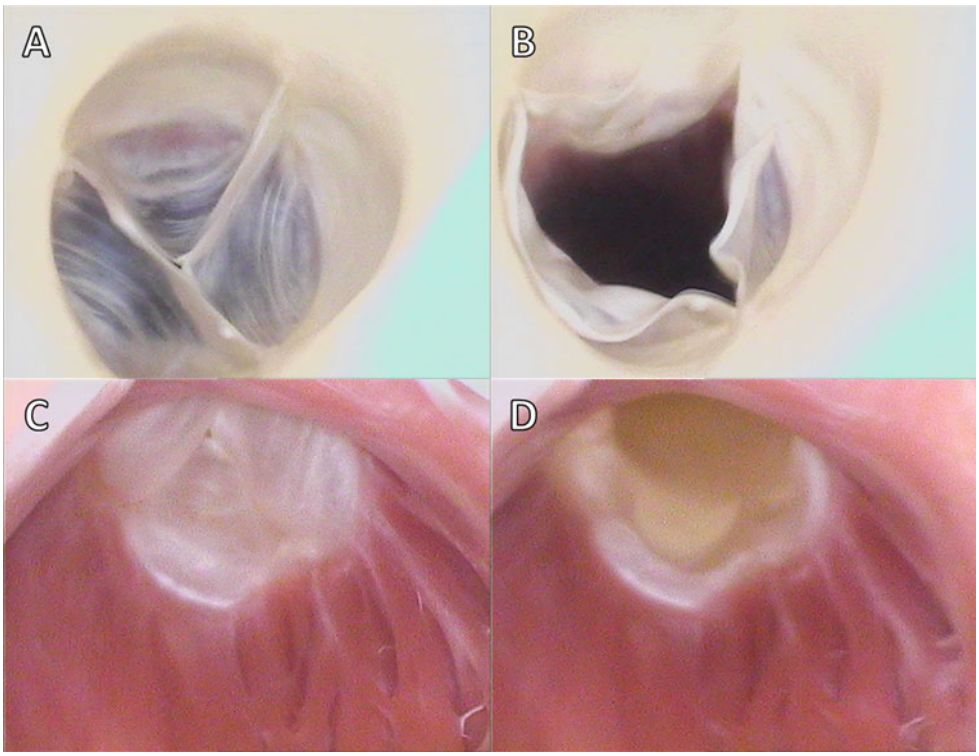

Fig. 7.7 Internal videoscopic images of the pulmonary valve from above (**a**, **b**) and below (**c**, **d**) during systole (**a**, **c**) and diastole (**b**, **d**) obtained employing Visible Heart® methodologies

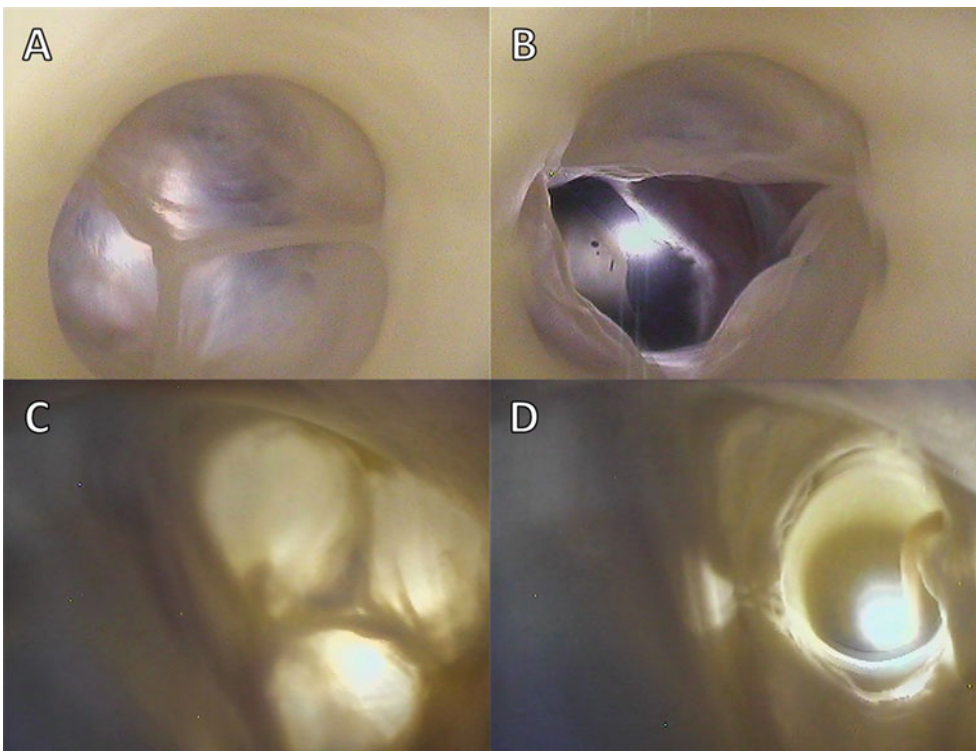

Fig. 7.8 Internal videoscopic images of the aortic valve from above (**a**, **b**) and below (**c**, **d**) during systole (**a**, **c**) and diastole (**b**, **d**) obtained employing Visible Heart® methodologies

Figures 7.7 and 7.8 show image sequences of the functional movements of the pulmonary and aortic valves, respectively; these images were obtained from reanimated human hearts employing Visible Heart® methodologies [17, 18]. The images include views of semilunar valves from above (i.e., from videoscopes within the pulmonary artery and the aorta) and from below (with videoscopes within the right and left ventricular outflow tracts).

In general, dysfunction of the semilunar valves is usually characterized by one of two symptoms: failure of the valves to successfully close or failure of the valves to successfully open. Dysfunction of the valves during systole, i.e., failure of the valve to successfully open, is defined as *stenosis* of the valve. This pathology is characterized by reduction in the effective orifice area of the valve (the size of the opening that allows blood to pass), which in turn forces the ventricles to work harder to move blood to the body or lungs. Dysfunction of the semilunar valves during diastole, when the ventricles are relaxing, results in *regurgitation*; this occurs when blood is allowed back into the ventricle from the arterial system, overloading the ventricles and potentially causing chronic heart failure.

7.5 Valve Histologies

Interestingly, the atrioventricular valves share very similar leaflet histology. The atrial sides of the leaflets consist of spongy tissue (lamina spongiosa) comprised of fibrocytes, histiocytes, and collagen fibers [22]. It is these collagen fibers that are considered to supply the mechanical strength required of the atrioventricular valves. The ventricular sides consist of fibrous tissue (lamina fibrosa), and both these layers are surrounded by endothelial cells. Additionally, the valve leaflets have been shown to incorporate both primary sensory and autonomic innervation. In general, it is considered that the anterior leaflet of the mitral valve has twice the innervation of the posterior leaflet [23]. These nerves are typically situated in the lamina spongiosa and extend over the proximal and medial portions of the leaflet [22]. Fibroblasts [24], smooth muscle cells [25, 26], and myocardial cells [27] are also commonly located within the leaflet tissue.

Cells within the leaflets have been shown to elicit two types of contractile activity: (1) a brief contraction or twitch at the beginning of each heartbeat (reflecting contraction of myocytes in the leaflet in communication with, and excited by, atrial muscle) which has relaxed by mid-systole and whose contractile activity is eliminated with β-receptor blockade, and (2) sustained tonic contractions (or tone) during isovolumic relaxation, which has been shown to be insensitive to β-blockade, but doubled by stimulation of the neurally rich region of aortic-mitral continuity [28]. These contractile activities within the leaflets are hypothesized to aid in the maintenance of anterior leaflet shape. This, in turn, could help prevent mechanical shock to the leaflets upon valve closure and also aid in optimizing the leaflet shape for funneling blood into the left ventricular outflow tract [28].

The tendinous cords are composed of a collagen core, surrounded by elastin fibers interwoven in layers of loose collagen. Similar to the valve leaflets, they also have an outer layer of endothelial cells, but it is the collagen cores that support the greatest degree of mechanical load during systole and allow for the wavy configuration during diastole. The elastin fibers are normally arranged in parallel fashion relative to the collagen fibers, and as the cords are stretched during systole, the elastin fibers are also stretched, straightening the collagen. It is hypothesized that it is this composite configuration of elastin and collagen that provides a smooth mechanism for the transmission of cordal forces from the leaflets to the papillary muscles. Additionally, during diastole, the stretched elastin fibers likely help to restore the wavy configuration of the primary collagen cores. The relative amount of collagen and elastin within the given chordae varies according to their relative types, as does the relative amount of contained DNA and their degree of vascularization. Normally the vascularization of the tendinous cords is located between their collagen cores and the elastin fibers and is further considered to supply nutrients to the leaflets. It has been reported that a higher DNA content within both the anterior and posterior marginal chordae relates to inherently higher rates of collagen syntheses in order to prevent mechanical deterioration compared with other types of chordae [13].

The papillary muscles can be considered part of the ventricular myocardium and hence are composed of aggregated myocytes. The cells exhibit complex junctions, called *intercalated discs*, allowing multiple cells to form long cellular networks. Within the papillary muscles, these muscle fibers run parallel to each other along the length of the muscle to increase contractile force and efficiency. The papillary muscles are extensively innervated and have complex vascular systems in order to maintain coordinated contractions with the continuum of the ventricular myocardium [29].

It was Gross who first drew attention to the specific histological structures of the arterial valves, his account then being endorsed by others such as Misfeld and colleagues [22, 30]. Each leaflet of the semilunar valve was described to have a fibrous core, or *fibrosa*, with an endothelial lining containing delicate sheets of elastin on its arterial and ventricular aspects. This so-called fibrous "backbone" is represented by a dense collagenous layer, which gives way to a much looser structure, or *spongiosa*, toward the ventricular aspects of the leaflet cusps. The zone of apposition of the leaflets consists of an abrupt thickening of the fibrous layer made up of closely packed vertically directed fibers and builds at the central portion of the free edge, creating a node termed the *nodulus Arantii* [22, 30]. Figure 7.9 displays a cross section of an aortic valve leaflet displaying the varying tissue types [31].

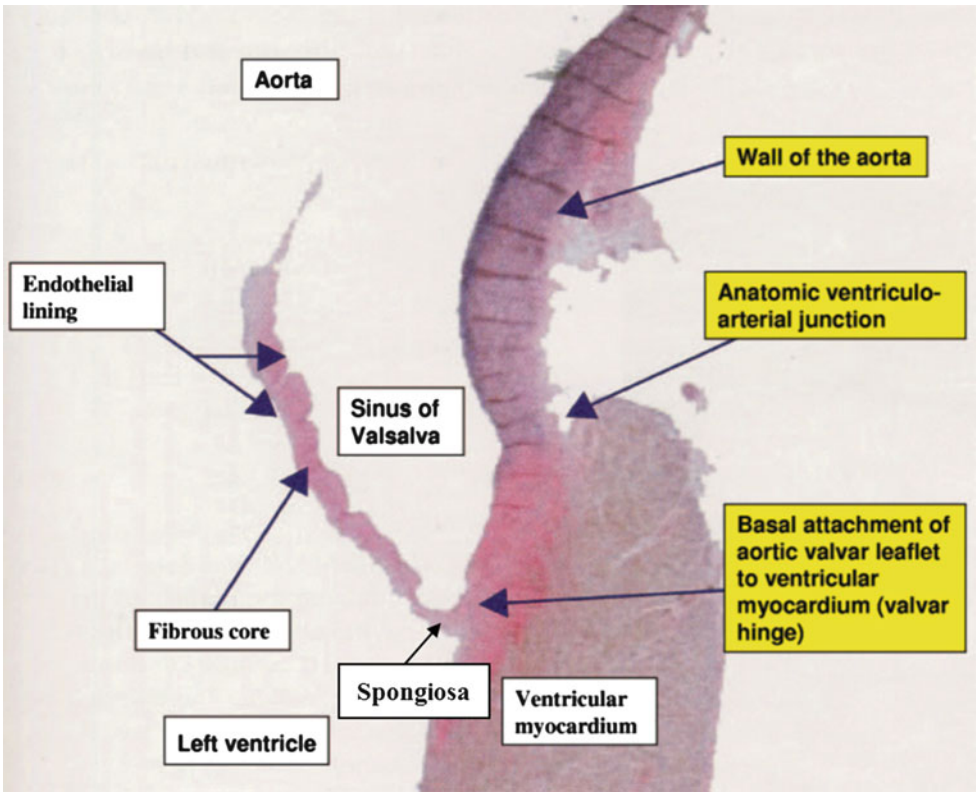

Fig. 7.9 Histologic features of the aortic valvar complex showing the anatomic ventriculoarterial junction. Also note that the basal attachment of the aortic valvar leaflets to the ventricular myocardium is proximal relative to the anatomic junction. Image is reproduced with permission from Piazza N et al. (2008) [31]

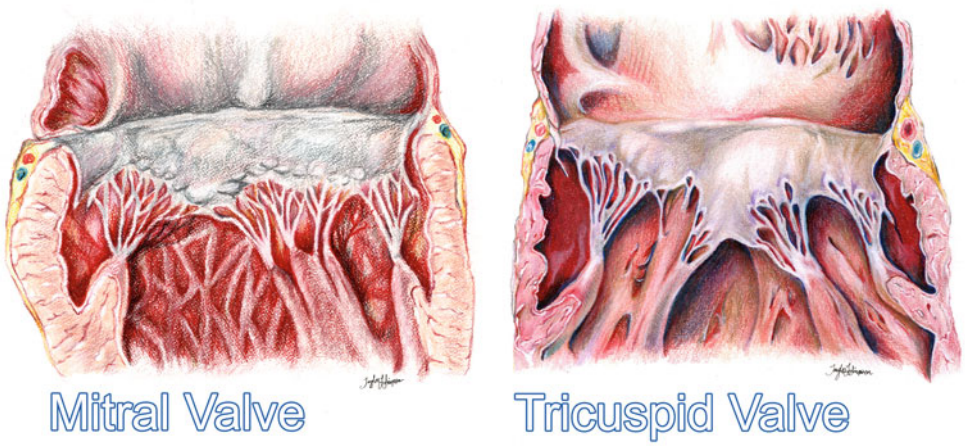

Fig. 7.10 An artist's rendition of the healthy mitral and tricuspid valves clearly showing the annuluses, leaflets, tendinous cords, and papillary muscles

7.6 The Mitral Valve

The left atrioventricular valve, or mitral valve, named by Andreas Vesalius due to its structural resemblance to the cardinal's mitre, is situated in the left atrioventricular junction and modulates the flow of blood between the left atrium and ventricle. Commonly, the valve consists of an annulus, two leaflets, two papillary muscle complexes, and two sets of tendinous cords, as seen in Fig. 7.10.

In 1976 Carpentier described the mitral valve as consisting of two apposing leaflets—a posterior leaflet with three scallops and an anterior leaflet with one scallop. Each region of the leaflets is designated an alphanumerical label to distinguish it from the rest of the valve (Fig. 7.11) [32]. However, when one considers these structures relative to the landmarks of the body (i.e., in an attitudinally correct nomenclature), the leaflets are located in posteroinferior and anterosuperior positions. Confusion regarding positional nomenclature can be avoided when adopting the more traditional approach suggested by Vesalius for distinguishing between the leaflets and recognizing that they are aortic and mural in their locations [33]; in this chapter, we will use such nomenclature. The

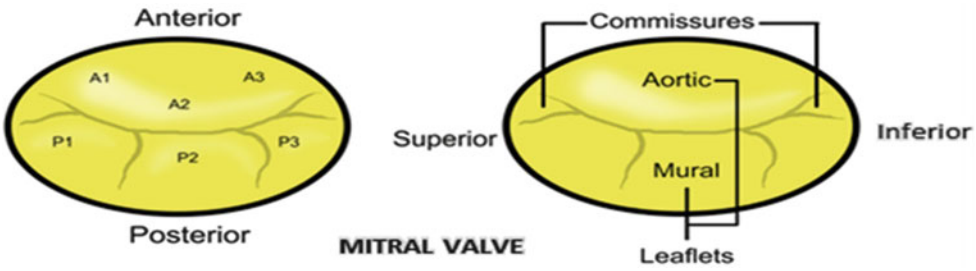

Fig. 7.11 Nomenclature of the mitral valve leaflets. The *left* diagram shows Carpentier's 1976 nomenclature, while the *right* depicts the modern attitudinally correct nomenclatures

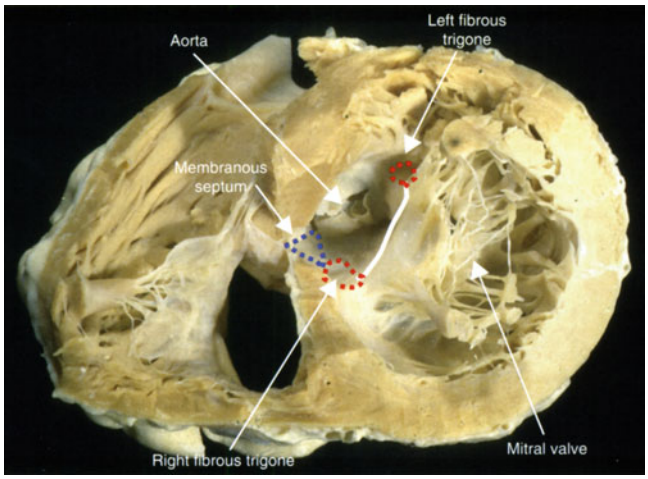

Fig. 7.12 Trigones and the aorto-mitral fibrous continuity within a sectioned human heart. In this case, the cardiac skeleton is being viewed from the apex of the heart. The anterior cardiac surface appears in the upper part of this image, whereas the posterior surface is below. Image is reproduced with permission from Anderson RH et al. (2006) [33]

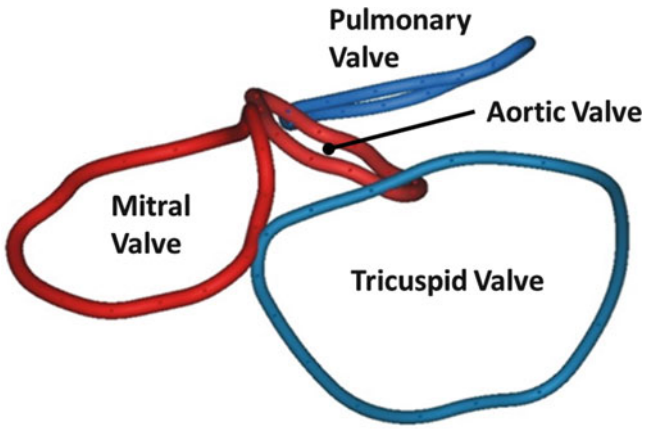

Fig. 7.13 3D reconstruction of the annuluses of the mitral (*red*) and tricuspid (*blue*) valves in Mimics® (Materialise, Leuven, Belgium) from CT scans of a human heart in vivo. The image also shows the location of the virtual rings formed by joining together the basal attachments of the leaflets of the aortic and pulmonary valves

junctions of the two leaflets are commonly referred to as the *anterolateral* and the *posteromedial* commissures; however, they are more accurately described as superior and inferior. The line of apposition of the leaflets during valve closure is known as the *fibrous ridge*. The simplicity and practicality of Carpentier's anatomic description of the mitral leaflets led to its widespread use after being introduced in 1976 [32]; yet, while this description depicts a majority of mitral valve anatomies, there can be wide variability in the number of scallops within each leaflet and their relative positions [34].

In general, the aortic leaflet is found to be attached to approximately one-third of the annulus circumference and is supported by the aorto-mitral fibrous continuity, which terminates in the left and right fibrous trigones (Fig. 7.12). The mural leaflet is attached to the remaining two-thirds of the annulus and also to the fibrous extensions that continue from the trigones around the mitral valve. However, the lengths of these extensions can be highly variable. Furthermore, a fibrous-fatty tissue surrounds the valve in areas where the cardiac skeleton is not present. The mitral annulus is a highly dynamic feature of the heart, changing dramatically in shape and size throughout the cardiac cycle. It is often described as being saddle-shaped with the highest point of the saddle, the *saddlehorn*, being found at the midpoint of the area of aortic-to-mitral valvar continuity [35] (Figs. 7.4 and 7.13). Both Delgado and Veronisi and their colleagues reported a series of annular dimensions that were recorded using echocardiography in healthy patients; these data are summarized in Table 7.1 [36–38].

Table 7.1 Data on the mitral valve annulus measured via CT [36] and 3D echocardiography [37, 38]

Measured anatomical feature	Data	Sample size
Systolic annular area [36, 37]	9.12 ± 1.71 cm^2 9.49 ± 1.25 cm^2	$n=84$ $n=13$
Septal-lateral (A2-P2) diameter [36, 37] (considered the short axis of the valve)	2.38 ± 0.40 cm 3.00 ± 0.45 cm	$n=84$ $n=13$
Commissure-commissure diameter [36, 37] (considered the long axis of the valve)	4.10 ± 0.48 cm 3.42 ± 0.40 cm	$n=84$ $n=13$
Annulus height during systole [38]	8.1 ± 1.7 mm	$n=24$

In general, the sub-valvar apparatus of the mitral valve consists of two adjacent papillary muscle complexes—the superoposterior (anterior or APM) and the inferoanterior

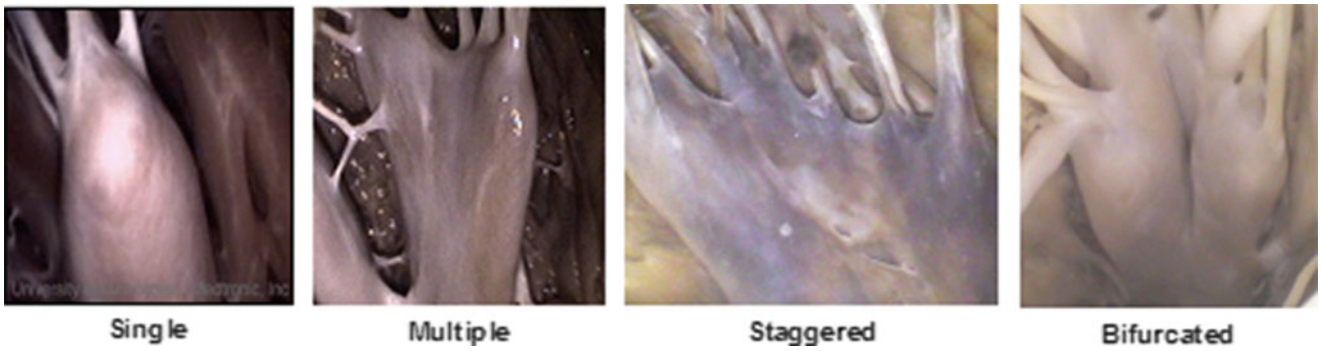

Fig. 7.14 Several representative examples of the enormous variation in anatomy with regard to the papillary muscle heads associated with the mitral sub-valvar apparatus from four different human hearts taken using Visible Heart® methodologies [40]

Table 7.2 Data on the chordal lengths of the mitral sub-valvar apparatus measured in vivo via 3D echocardiography [41] and post mortem [42, 43]

Measured anatomical feature	Data	Sample size
APM tethering length in systole [41]	3.54 ± 0.82 cm	n = 120
PPM tethering length in systole [41]	3.76 ± 0.78 cm	*n* = 120
Anterior leaflet insertion length [42]	1.81 ± 0.49 cm	*n* = 50
Posterior leaflet insertion length [42]	1.18 ± 0.26 cm	*n* = 50
Ratio of chordal origins to insertions [43]	1:5	*n* = 18

APM superoposterior (anterior) papillary muscle

PPM inferoanterior (posterior) papillary muscle

(posterior or PPM)—with their attached tendinous cords which, in turn, insert onto the ventricular surfaces of each of the two valve leaflets [33]. In other words, the superoposterior papillary muscle complex is not solely associated with the aortic leaflet, but rather both the leaflets; likewise, the inferoanterior papillary muscle complex is not solely associated with the mural leaflet. It is important to note that the morphologies of the papillary muscle complexes are highly variable [36]. Some have proposed a complicated alphanumeric classification to account for the number of heads within each muscle and the number of attachments with the ventricular walls [39]. Even this complex code can be deemed as an oversimplification, as both papillary complexes can exhibit enormous anatomic variation [40]. For example, Fig. 7.14 displays images of the sub-valvar apparatus of the mitral valve taken from human hearts in the Visible Heart® library [40].

The tendinous cords are typically classified by their number and length and quantified by one of two measurement techniques—tethering length and insertion length. *Tethering length* is defined as the distance from the papillary head to the saddlehorn of the mitral annulus. *Insertion length* is defined as the length of the cords from their origin at the papillary head to their insertion into the leaflet tissue. Anatomical dimensions obtained from patients with no reported mitral regurgitation or other valvar pathologies were reported by Sonne et al. and Lam et al. and are summarized in Table 7.2 [41, 42]. Yet, it should be emphasized that, as with other anatomical studies, these data do not account for all anatomical variations. For example, it has also been reported that the cordal attachments to the mural leaflet may extend simply from the ventricular myocardium to the leaflet without a papillary muscle attachment. Furthermore, it is well known that the tendinous cords themselves may elicit highly variably anatomies, and various subpopulations of chordae have been classified by both function [43] and type [44]. Figure 7.15 shows examples of these identified variations in the types of chordae, including posterior marginal chordae, commissural chordae, anterior strut chordae, anterior marginal chordae, basal posterior chordae, and posterior intermediate chordae.

7.7 The Tricuspid Valve

The right atrioventricular valve, or tricuspid valve, is situated within the right atrioventricular junction and modulates the flow of blood between the right atrium and right ventricle. This valve is typically defined by three leaflets suspended from the muscular atrioventricular junction and connected to the ventricular wall via three distinct papillary muscle complexes (as seen in Fig. 7.10). When defined using attitudinally correct nomenclature, these leaflets are located in septal, anterosuperior (traditionally anterior), and inferior (traditionally posterior) positions (Figs. 7.16 and 7.17) [45].

The anterosuperior leaflet is the largest of the three and extends from the medial border of the ventricular septum to the acute margin of the atrioventricular junction (Fig. 7.15). The leaflet is hinged from the undersurface of the supraventricular crest and provides a curtain between the inflow and outflow tracts of the right ventricle. The inferior leaflet is hinged from the diaphragmatic aspect of the atrioventricular junction. The septal leaflet is then hinged from the ventricular border of the triangle of Koch, with the hinge crossing the right-sided aspect of the membranous septum, dividing it into atrioventricular and ventriculoarterial components [46]. The septal leaflet is often cleft as it crosses the membranous

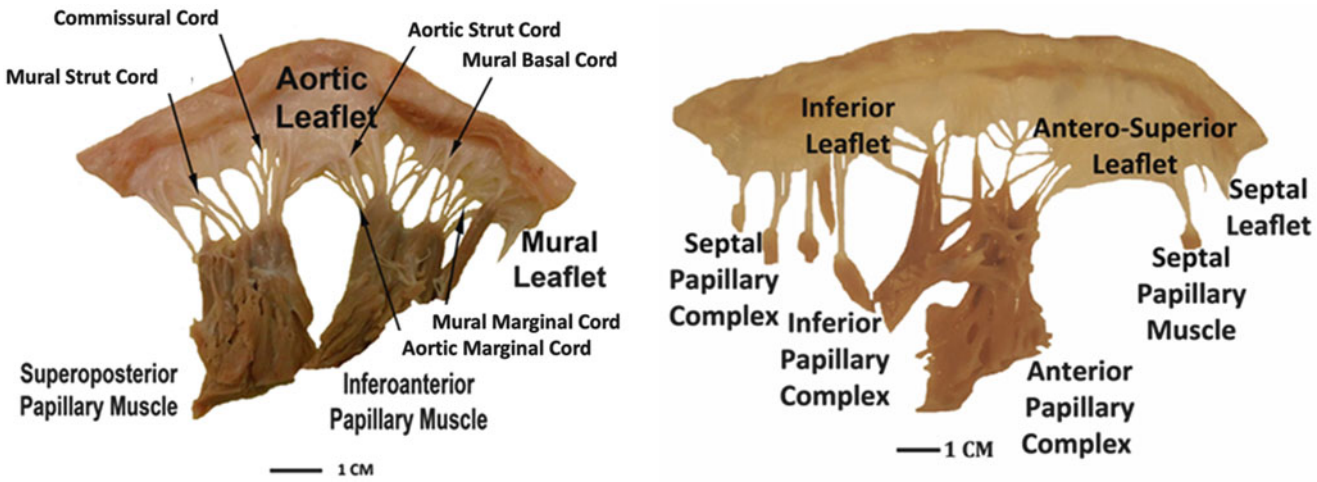

Fig 7.15 Dissections of a human mitral valve (*left*) and tricuspid valve (*right*), each labeled with attitudinally correct nomenclature. Note the dramatic differences between the two valves, including their respective sub-valvar apparatuses

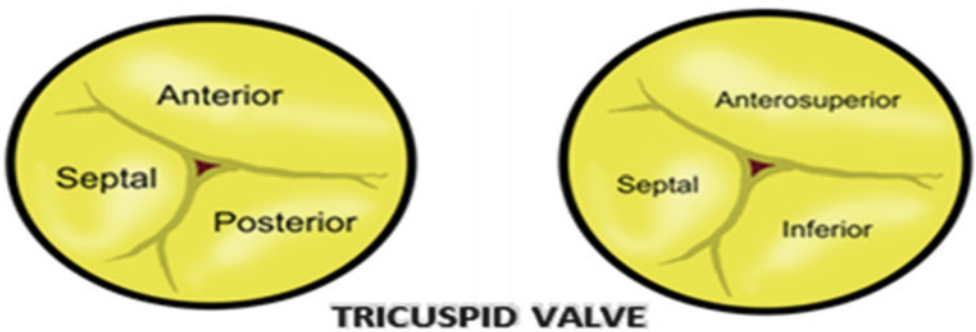

Fig. 7.16 Nomenclature of the tricuspid valve leaflets. The *left* diagram shows Carpentier's 1976 nomenclature, the *right* depicts the modern attitudinally correct nomenclatures

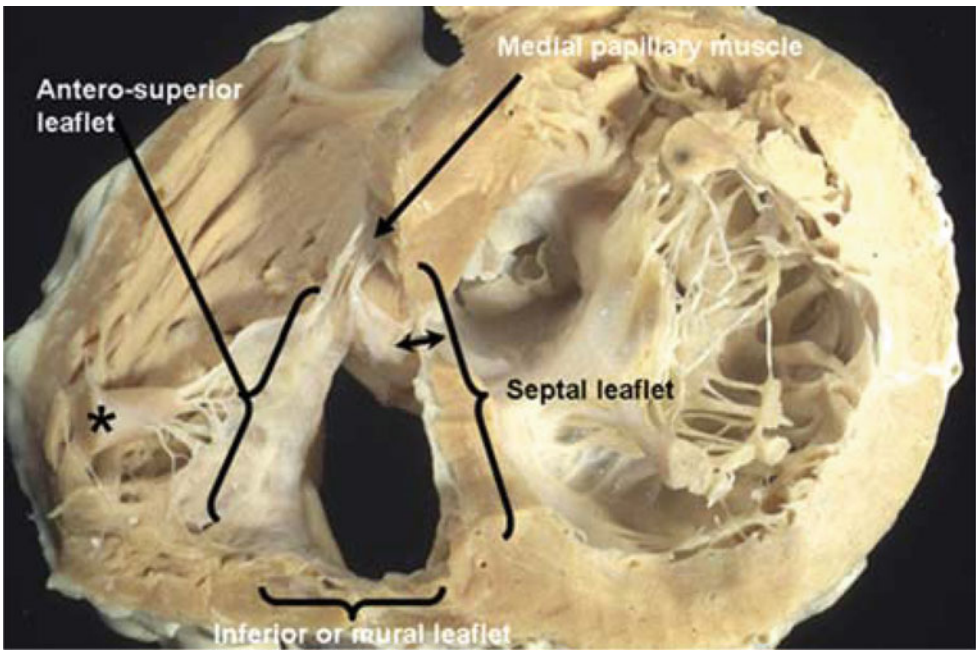

Fig. 7.17 Relative positions of the three leaflets of the tricuspid valve positioned septally, anterosuperiorly, and inferior or murally. Note the location of the membranous septum as indicated by the *double-headed arrow*. In this human heart, the anterior papillary muscle (*asterisk*) is attached to the midpoint of the anterosuperior leaflet. Image is reproduced with permission from Martinez RM et al. (2006) [45]

septum. When viewed in closed position, the trifoliate zones of apposition between the leaflets extend to their peripheral ends. It is these ends that are typically considered to represent the valvar commissures, which can be named as being anteroseptal, anteroinferior, and infero-septal [2].

To date, the morphology of the tricuspid valve has received less attention than the mitral valve; hence, thorough anatomical studies are limited. The tricuspid annulus is known to have a non-planar three-dimensional shape, similar to the mitral valve annulus (Fig. 7.13). Further, it has been described as changing its shape dramatically throughout the course of the cardiac cycle. These changes in annular geometry during systole, from a more circular shape to an elliptical shape, result in overall reduction of annular sizes by up to 40 % [47]. As the heart contracts, the annulus reaches its minimum size during isovolumetric relaxation and its maximum during isovolumetric contraction [35]. Data relating to the tricuspid annulus can be seen in Table 7.3 [37, 48–50].

As with the mitral valve, the leaflets of the tricuspid valve are complimented by a sub-valvar apparatus consisting of papillary muscle complexes that work to tether the valve leaflets via tendinous cords to prevent valve prolapse during ventricular contraction (systole). The three main papillary muscle complexes have grossly dissimilar morphology, albeit very characteristic (Fig. 7.18). The zone of apposition between the septal and anterosuperior leaflets is supported by the medial papillary muscle complex, also known as the papillary muscle of the conus, or the muscle of Lancisi [45, 51]. It arises from the posteroinferior limb of the septal band, or septomarginal trabeculation, although in some individuals the muscle is replaced by a series of smaller muscles or even by cords arising directly from the septal band. The anterior is typically the largest papillary muscle complex and supports the zone of apposition between the anterosuperior and inferior leaflets, but often inserts into the midportion of the anterosuperior leaflet. The muscle itself is usually in direct continuity with the moderator band [46]. This latter structure is one of a series of septoparietal trabeculations that arise from the anterior margin of the septal band. The smaller inferior muscle complex supports the zone of apposition between the inferior and septal leaflets. The septal leaflet is then supported in addition by multiple cords arising directly from the septum itself. This is a differentiating feature between the tricuspid and mitral valves, the leaflets of the latter valve lacking any septal attachments.

Figure 7.18 displays videoscopic images of the sub-valvar apparatus of the tricuspid valve taken from reanimated human hearts utilizing Visible Heart® methodologies, as described in Chap. 41. Such images emphasize the large anatomical variations that can exist from heart to heart (unpublished data).

Previously, Silver et al. reported the common insertion length of the tendinous cords of the tricuspid valve for healthy human hearts, which was defined as the distance from the origin of the papillary muscles to their corresponding insertion points on the valve leaflets (Table 7.4) [49]. These measurements were completed on 50 formalin-fixed human hearts; it should be noted that these data may have

Table 7.3 Data on the mitral valve annulus measured in vivo via 3D echocardiography [37] and post mortem [48–50]

Measured anatomical feature	Data	Sample size
Systolic annular area [37]	10.75 ± 1.81 cm^2	$n = 13$
Post mortem orifice area [48]	10.60 ± 3.40 cm	$n = 160$
Systolic septo-medial dimension [37]	3.31 ± 0.32 cm	$n = 13$
Systolic anterior-posterior dimension [37]	3.79 ± 0.43 cm	$n = 13$
Postmortem annular circumference [49, 50]	11.10 ± 1.10 cm 11.30 ± 0.50 cm	$n = 50$ $n = 24$

Table 7.4 Data on the chordal lengths of the tricuspid sub-valvar apparatus measured post mortem [49]

Measured anatomical feature	Data (cm)	Sample size
Septal leaflet insertion length [49]	1.50 ± 0.87	$n = 50$
Anterior leaflet insertion length [49]	1.53 ± 0.69	$n = 50$
Posterior leaflet insertion length [49]	1.37 ± 0.64	$n = 50$

Fig. 7.18 Several representative examples of the septal (*left*), inferior (*center*), and anterior (*right*) papillary muscle complexes associated with the tricuspid sub-valvar apparatus taken using Visible Heart® methodologies (unpublished data)

specific limitations when compared to the modern imaging techniques, e.g., those used to measure the tethering length of the mitral cords mentioned earlier in the chapter. As such, we suggest that future detailed assessments of the tricuspid sub-valvar apparatus employing modern imaging techniques could greatly benefit the field.

7.8 The Aortic Valve

As previously mentioned, due to its location in the center of the heart between the mitral valve and the tricuspid valve, the aortic valve is considered as the "centerpiece" of the heart and is often the most important cardiac valve with respect to normal cardiac function [31]. An artist's rendition of the opened aortic root showing the features of the aortic valve can be seen in Fig. 7.20.

7.8.1 The Aortic Root

The aortic root contains three circular rings and one crown-like ring (Fig. 7.6) [19]. The connection of the leaflets to the arterial wall mimics the shape of a crown, whose base forms a virtual ring known as the basal plane of the valve. This plane represents the inlet from the left ventricular outflow tract into the aortic root. The top of the crown can be considered as a true ring, the sinotubular junction, defined by the sinus ridge and the related sites of attachment of the peripheral zones of apposition, between the aortic valve leaflets [31]. Hence the sinotubular junction dictates the transition from the aortic root into the ascending aorta. The semilunar hinges then cross another defined "ring" known as the anatomic *ventriculoarterial* junction. This overall anatomic arrangement was illustrated previously in Fig. 7.6, but can be readily observed when the aortic root is opened linearly as seen in Fig. 7.19.

The normal aortic root elicits a relatively consistent shape between patients, but can vary dramatically in size (Table 7.5) [29, 52]. Kunzelman et al. demonstrated a definable mathematical relationship between root diameter and clinically

Table 7.5 Data on the aortic valve annulus, sinus of Valsalva, and sinotubular junction measured using multislice computed tomography

Measured anatomical feature	Data (mm)	Sample size
Maximum aortic annular diameter [52, 29]	26.9 ± 2.8 26.4 ± 2.8	$n = 25$ $n = 150$
Minimum aortic annular diameter [52, 29]	21.4 ± 2.8 24.0 ± 2.6	$n = 25$ $n = 150$
Sinus of Valsalva mean diameter [29]	32.3 ± 3.9	$n = 150$
Sinus of Valsalva height above the basal plane [29]	17.2 ± 2.7	$n = 150$
Sinotubular junction mean diameter [29]	28.1 ± 3.1	$n = 150$
Sinotubular junction height above basal plane [29]	20.3 ± 3.1	$n = 150$

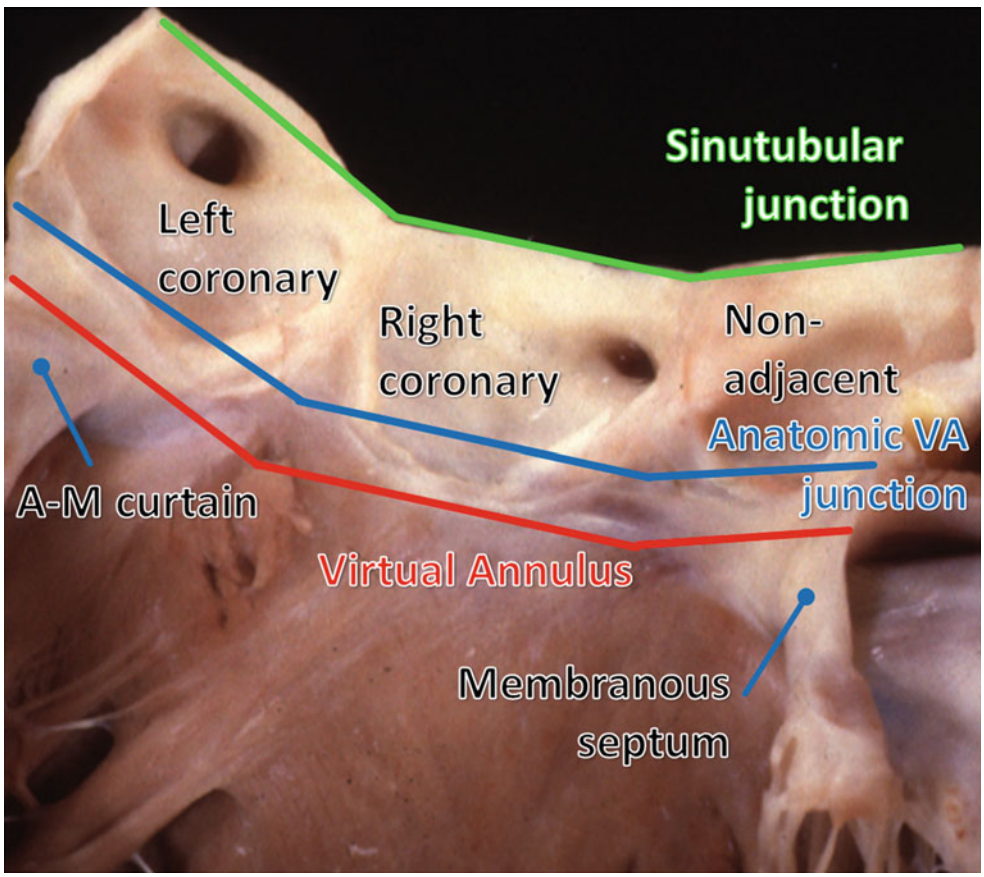

Fig. 7.19 The aortic leaflets have been removed from this human aortic root specimen. One can then observe the locations of the three defined aortic rings, i.e., relative to the crown-like hinges of the leaflets. *A-M* aortic-mitral, *VA* ventriculoarterial [7]. Image was modified from an original figure provided by Professor Robert H. Anderson; Professor Anderson retains the intellectual copyright of the original image

measurable leaflet dimensions [53]. In general, the diameter at the level of the sinotubular junction typically exceeds that at the level of the basal plane by a factor of 1:1.6 [53, 54]. The valvar complex is a dynamic structure with its geometric parameters changing continuously throughout the phases of the cardiac cycle and relative to the associated changes in pressure that will occur within the aortic root [55]. For example, from diastole to systole, the relative change in diameter at the level of the sinotubular junction and at the *ventriculo-arterial* junction has been noted to increase by ~12 % and decrease by ~16 %, respectively [56–58]. Additionally, the orientation of the left ventricular outflow tract and the aortic root (i.e., the angle between the two) is known to vary from patient to patient. It is also understood that this angle becomes more acute with age. Middelhof et al. reported that hearts from individuals aged >60 years exhibited angles between 90° and 120°, whereas individuals aged <20 years presented with angles between 135° and 180° [59].

It is important to note that one of the most critical functions of the aortic root is to facilitate coronary artery perfusion during ventricular diastole. This is achieved by directing 3–5 % of the circulating blood through both the left and right coronary arteries while the aortic valve itself is closed. In general, the orifices of the coronary arteries arise within the two anterior sinuses of Valsalva, usually positioned just below the sinotubular junctions [54, 60, 61]. However, it is not unusual to find these arteries positioned superior relative to the sinotubular junction. Cavalcanti et al. reported the mean distance measured from the orifice of the left coronary artery to the basal attachments of the corresponding leaflets was 12.6 ± 2.61 mm, and for the right coronary artery, it was 13.2 ± 2.64 mm in 51 normal postmortem hearts [62]. Variations in coronary arterial origin, nonetheless, can occur with some of these configurations posing as risk factors in sudden cardiac death [63, 64]. It should also be recalled that it is the location of these coronary arteries that dictates the naming of the aortic valve leaflets/cusps—the left coronary, the right coronary, and the nonadjacent (or non-coronary).

7.8.2 The Aortic Leaflets

As noted above, the leaflets of the aortic valve are named for the branching coronary arteries that feed the left and right sides of the heart (Fig. 7.20). More specifically, both the right and left leaflets attach to the aortic root in the predominantly muscular region of the left ventricular outflow tract, whereas the nonadjacent leaflet is chiefly attached to the fibrous region above the membranous septum (Fig. 7.19). This fibrous continuity connects the aortic valve to the anterior (aortic) leaflet of the mitral valve, forming the aortic-mitral curtain. The zone of apposition of the right leaflet to the nonadjacent leaflet is positioned above the membranous part of the ventricular septum. The zone of apposition of the nonadjacent leaflet with the left coronary aortic leaflet is adjacent to the anterior wall of the left atrium. The left leaflet

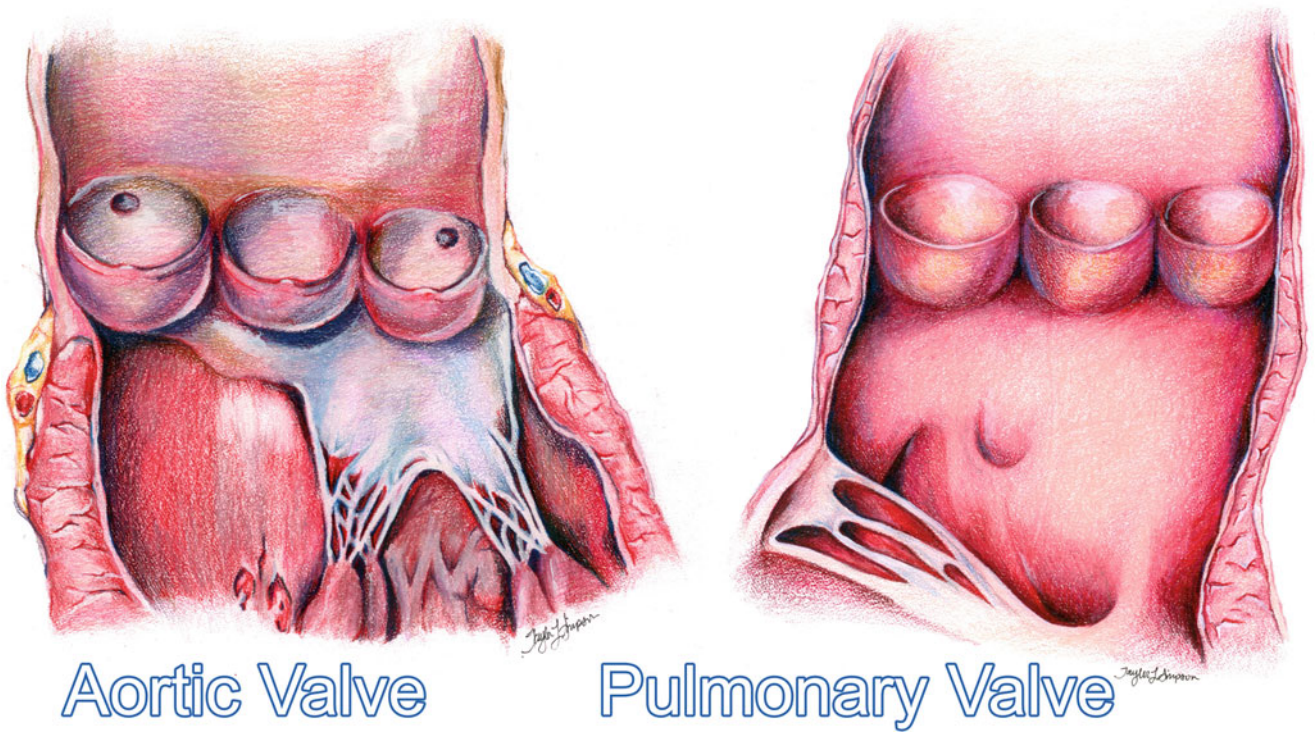

Fig. 7.20 Artist's rendition of the healthy aortic and pulmonary valves clearly showing the leaflets, sinuses, outflow tracts, and arterial trunks

then continues toward the right leaflet, again achieving support from the muscular part of the ventricular septum. As previously mentioned, the zones of apposition themselves ascend as they extend to be attached peripherally at the sinotubular junction; below each peripheral attachment, there is a fibrous interleaflet triangle that forms part of the ventricular outflow tract [65].

It should be noted that variations may exist in all dimensions of individual leaflets, including: (1) height, (2) width, (3) surface area, and (4) volume of their supporting sinuses of Valsalva [31]. Vollebergh et al. reported that the average widths (measured between the peripheral zones of attachment along the sinus ridge) for the right, the nonadjacent, and the left coronary leaflets were 25.9, 25.5, and 25.0 mm respectively, in an investigation of 200 normal hearts [66]. It was also described that the average heights (measured from the base of the center of the leaflet to their free edges) for the right coronary, nonadjacent, and left coronary cusps were 14.1, 14.1, and 14.2 mm, respectively. Such variations in the leaflet dimensions of healthy valves highlight the need to focus on the anatomy and function of each leaflet when developing prosthesis for either the surgical or transcatheter treatment of aortic valve pathologies.

7.9 The Pulmonary Valve

Due to its relative location within the infundibular musculature (at the distal portion of the right ventricular outflow tract), the pulmonary valve is considered, in an anatomical sense, a more simple valvar structure than the aortic valve (Fig. 7.20). The left and the right leaflets of the aortic valve face lie adjacent to the pulmonary trunk, and this relative anatomic orientation has been used to name the pulmonary valve leaflets: the right and left facing leaflets and the nonfacing leaflet (Fig 7.21) [1]. Anatomically, the commissure of both the right and left leaflets is supported by the supraventricular crest of the right ventricle, which separates the pulmonary valve from the tricuspid valve. Further, the opposite edge of the valve (i.e., the nonfacing leaflet is supported by the anterior wall of the infundibulum) is, in general, the most anterior part of the heart [1].

Pulmonary valve replacement is considered to be less challenging than aortic valve replacement due to the lower pressure gradient across the valve and the relative ease of access to the valve annulus. The ease of complete valve removal from the cardiac base has led to the use of an autograft replacement for the aortic valve in some congenital heart patients. Even so, information on the valve is less abundant and reports on variations in valve dimensions are less comprehensive. Capps et al. report the mean diameter of the valve as 25.4 ± 3.2 mm in a study comparing the size of the aortic and pulmonary valve to the overall body surface area (Table 7.6) [67]. It should be noted that these measurements were taken on valves removed postmortem using a Hegar dilator without annular dilation. By the authors' admission,

Table 7.6 Postmortem mean pulmonary and aortic diameters

Measured anatomical feature	Data (mm)	Sample size
Mean annular diameter [28]	25.4 ± 3.2	$n = 3997$
Mean aortic annular diameter [28]	22.4 ± 2.7	$n = 3370$

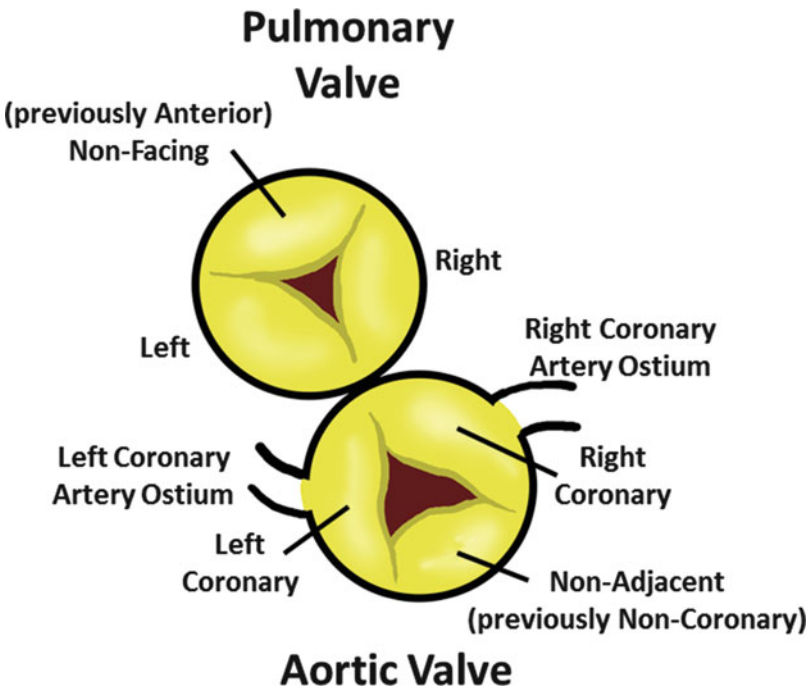

Fig. 7.21 Nomenclature for the individual leaflets of the aortic and pulmonary valves. The traditional naming system is displayed to the *left* and the updated attitudinally correct nomenclature to the *right*

this sizing presents limitations regarding the material properties of the pulmonary annulus differing significantly from the aortic [67]. As such, these measurements should be used as a rough guideline. The alternate methodology explains the difference in aortic measurements reported here from those measured at end systole in vivo by Schultz et al. and Tops et al. [20, 68], as shown in Table 7.5.

7.10 Valve Co-location with Other Cardiac Structures

When performing cardiac valve surgeries and/or contemplating novel percutaneous approaches to valvar repairs, it is vital to have a strong anatomical appreciation of the associated structures, i.e., those cardiac structures that surround the valves. The anatomical features surrounding the mitral and tricuspid valves are displayed in Figs 7.22 and 7.23. The position and course of the coronary vasculature is key to the clinical anatomy of both the mitral and tricuspid valves. The great coronary vein, continuing as the coronary sinus, circles the mural leaflet of the mitral valve [35, 69]. The circumflex artery, having branched from the main stem of the left coronary artery, courses in concert with the venous channel, usually running much closer to the hinge of the mural leaflet. In the majority of individuals with dominance of the right coronary artery, the circumflex artery does not extend through the full length of the left side of the inferior atrioventricular groove [35]. In the minority of individuals with left coronary arterial dominance, in contrast, the artery is directly related to the entirety of the mural leaflet, usually continuing into the floor of the triangle of Koch, where it gives rise to the artery supplying the atrioventricular node. In many individuals, the circumflex artery crosses underneath the coronary sinus at variable distances [33, 35, 69–71]. Both arterial and venous structures, therefore, are at risk when surgical procedures are performed on the mural leaflet of the mitral valve. Such considerations are particularly relevant when employing complex reconstructive techniques [35]. The proximity of the aortic valve is of importance when considering surgical procedures to the aortic leaflet of the mitral valve (Fig. 7.22). The interleaflet triangle between the left coronary and non-coronary (non-adjacent) aortic leaflets is directly related to the saddlehorn of the mitral valvar annulus. This feature should be remembered if sutures are to be placed to either side of the saddlehorn to prevent damage to the aortic valvar leaflets [35]. The tricuspid valve is bordered within the atrioventricular junction by the right coronary artery, but is less related to venous structures, the small cardiac vein being a relatively insignificant structure [7].

The atrioventricular node and its zones of transitional cells are closely related to the septal hinge of the tricuspid valve, with the slow pathway into the node being a constituent part of the vestibular atrial myocardium in this region. At the apex of the triangle of Koch [7, 35], the spe-

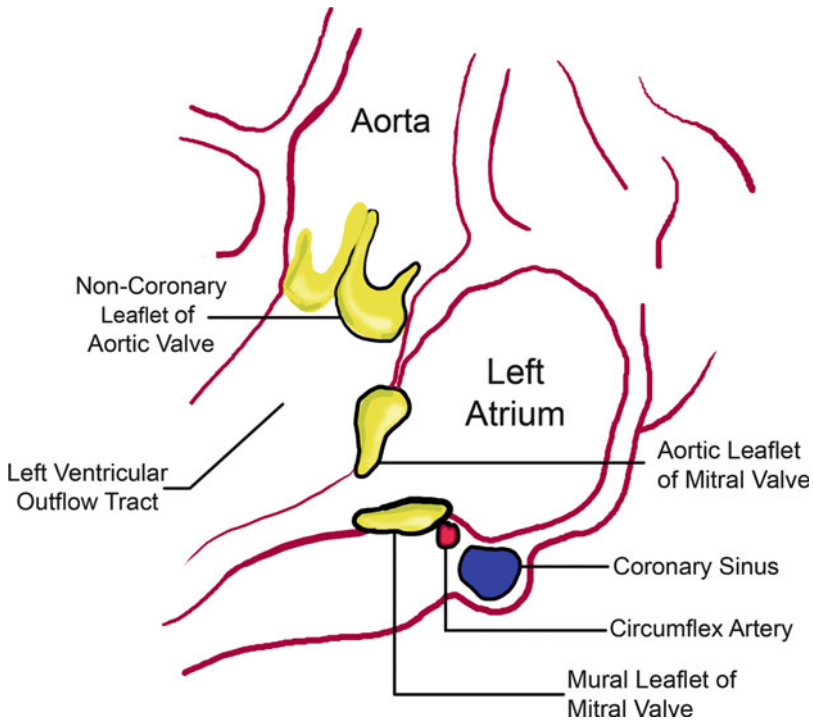

Fig. 7.22 Graphic representation of the co-location of the mitral valve to the coronary sinus, the left circumflex artery, and the aortic valve

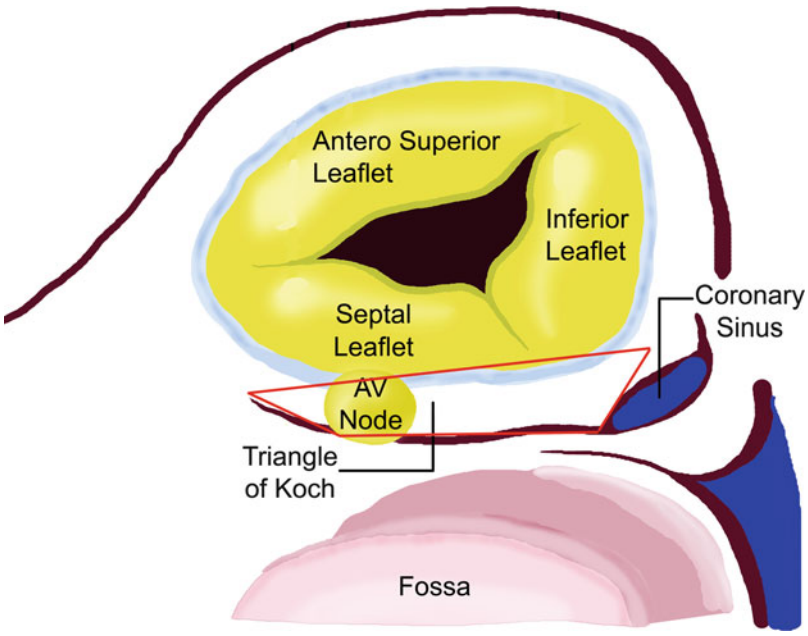

Fig. 7.23 Graphic representation of the relationship between the cardiac conduction system (i.e., the location of the atrioventricular node within the triangle of Koch) and the tricuspid valve when viewed from the right atrium

cialized cardiomyocytes of the atrioventricular node bundle themselves together and pierce the central fibrous body to become the penetrating atrioventricular bundle, or the bundle of His (Fig. 7.23). Although closely related again to the hinge of the septal leaflet of the tricuspid valve, and at potential risk whenever surgery is performed within the right atrium or through the tricuspid valve, the atrioventricular node should be sufficiently distant not to pose a threat to those operating on the mitral valve. The bundle of His, having passed through the membranous septum, divides on the crest of the muscular ventricular septum into the left and right bundle branches. These components are at greater risk during procedures on the aortic rather than the atrioventricular valves.

The most important anatomical structure related to the pulmonary root is the first perforating branch of the anterior interventricular artery; this artery is avoided during the Ross procedure. Note should also be taken of anomalous coronary arteries either coursing between the arterial roots or extending across the right ventricular infundibulum. Being located in the most anterior aspect of the heart, the pulmonary root is also directly adjacent to the sternum; thus, sternal compression may alter the performance of any prosthesis placed in the pulmonary annulus [4].

The anatomical orientation of the aortic valve is considered much more challenging; thus, the remainder of this section will focus on this valve. One of the most important and complex structures in proximity to the aortic valve is the *cardiac conduction system*. As mentioned previously, the atrioventricular node is located within the *triangle of Koch*, situating the atrioventricular node in close proximity to the subaortic region of the left ventricular outflow tract, helping to explain why the treatment of pathologies involving the aortic valve may lead to either a complete heart block or to an intraventricular conduction abnormality [31]. Further, as the atrioventricular conduction axis reaches the crest of the muscular ventricular septum, it then branches, with the left bundle branch cascading down the left ventricular septal surface, as illustrated so elegantly by Tawara over a century ago [72] (Fig 7.24).Thus, it is important that this anatomical relationship be considered when planning the repair and/or replacement of the aortic valve, as the interaction of a specific percutaneous prosthesis or the errant placement of sutures during surgical valve implantation can induce adverse effects on the conduction system and result in the patient requiring cardiac rhythm management.

In addition to the conduction system, an intimate knowledge of the aortic valve's proximity to both the coronary arteries and the mitral valve helps to minimize procedural complications.

In particular, the main stem of the left coronary artery can be remarkably short, bifurcating into the left anterior descending and circumflex arteries in close proximity to the root [4]. In the instance of transcatheter valve deployment, the prosthesis typically will crush the leaflets of the native valve against the aortic wall. Consequently, the combination of a relatively low-lying coronary artery ostium and a large, heavily calcified native aortic leaflet can lead to obstruction of the flow into the coronary arteries [31].

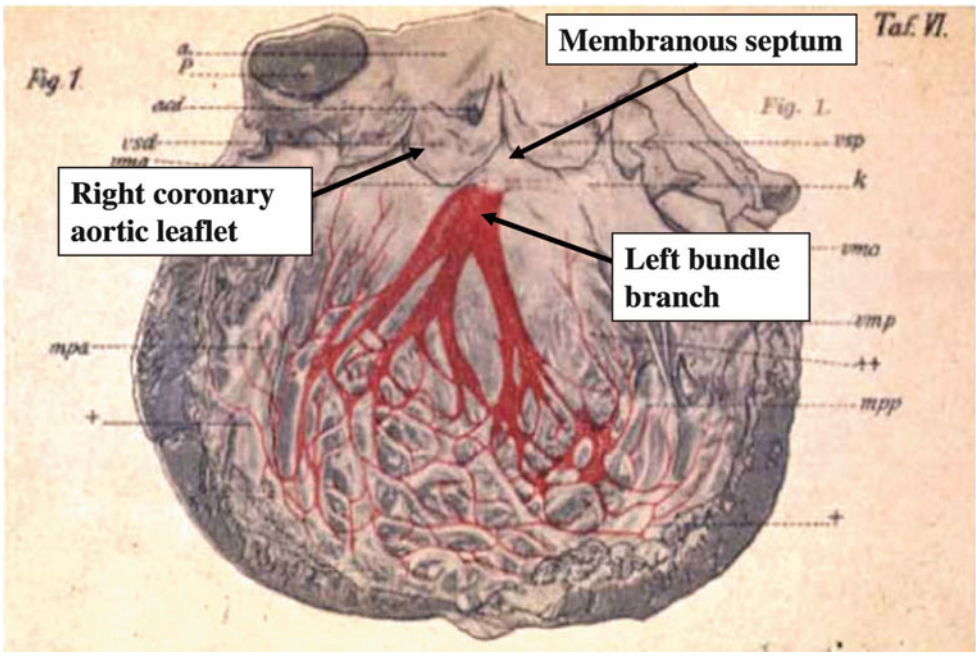

Fig. 7.24 Tawara's anatomical diagram of the left bundle branch showing the conduction system exiting from the base of the aortic valve between the nonadjacent and right coronary leaflets. It then branches out and descends along the septal endocardial surfaces of the left ventricular myocardium [9, 25]

7.11 Common Clinical Imaging of the Cardiac Valves

Due to its relatively high availability, ease of use, and minimal side effects to the patient, the standard 2D cross-sectional Doppler echocardiogram is considered as the most common imaging modality applied to assess the relative function and anatomical position of the cardiac valves [43, 73]. Clinically, both the mitral and tricuspid valves are commonly imaged via the parasternal long-axis view, allowing the echocardiographer to assess the following valve criteria [73]:

- Size and shape of the annulus
- Mobility of the leaflets, in particular, whether they prolapse or show flail or restricted motion (assessment will also include exclusion of thickening calcification, myxomatous degeneration, clefts, fusions along zones of apposition, perforations, vegetations, or abnormal shelves or membranes)
- Length and thickness of the tendinous cords and whether they are fused or ruptured
- Number, structure, and function of the papillary muscles
- Whether the function of the left ventricle is normal, is globally deranged, or shows evidence of regional abnormalities of motion of the walls

Examples of standard 2D cross-sectional Doppler echocardiograms of the mitral and tricuspid valve can be seen in Fig. 7.25.

The aortic valve can be readily viewed with echo from the apical, parasternal long-axis, and suprasternal views, whereas the pulmonary valve is usually imaged from the parasternal long-axis view (Fig. 7.26), allowing the echocardiographer to assess the following valve criteria [73]:

- Relative size and shape of the annulus.
- Number and mobility of the leaflets, in particular whether they show restricted motions. This assessment will also include exclusion of thickening calcification, fusions along zones of appositions, and/or leaflet damage.

For a comprehensive description of the echocardiographic techniques used to image and assess both healthy and diseased atrioventricular valves, the readers are referred to the *Textbook of Clinical Echocardiography* by Otto [74] and recommendations for clinical evaluation of stenosis by Baumgartner et al. [75] and regurgitation by Zoghbi et al. [76].

7.12 Summary

The atrioventricular and semilunar valves are highly complex anatomical structures. Their overall function and/or subsequent dysfunction can be due to abnormalities or failures within any of their respective subcomponents. Today, the detailed assessment of their anatomy and function, to determine optimal treatments approaches, provides critical information required by cardiologists, internationalists, and/or cardiac

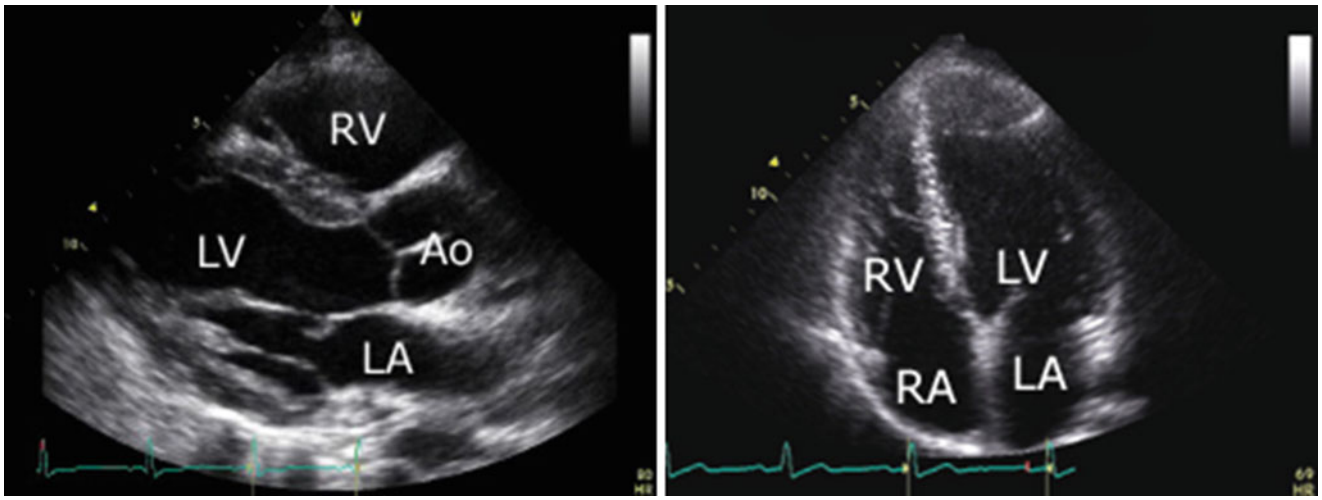

Fig. 7.25 Common echocardiographic parasternal long-axis and apical sections which show the leaflets of the mitral and tricuspid valves. The sub-valvar apparatus can clearly be seen tethering the leaflets to the ventricular free wall. *AO* aorta, *LA* left atrium, *LV* left ventricle, *RA* right atrium, *RV* right ventricle

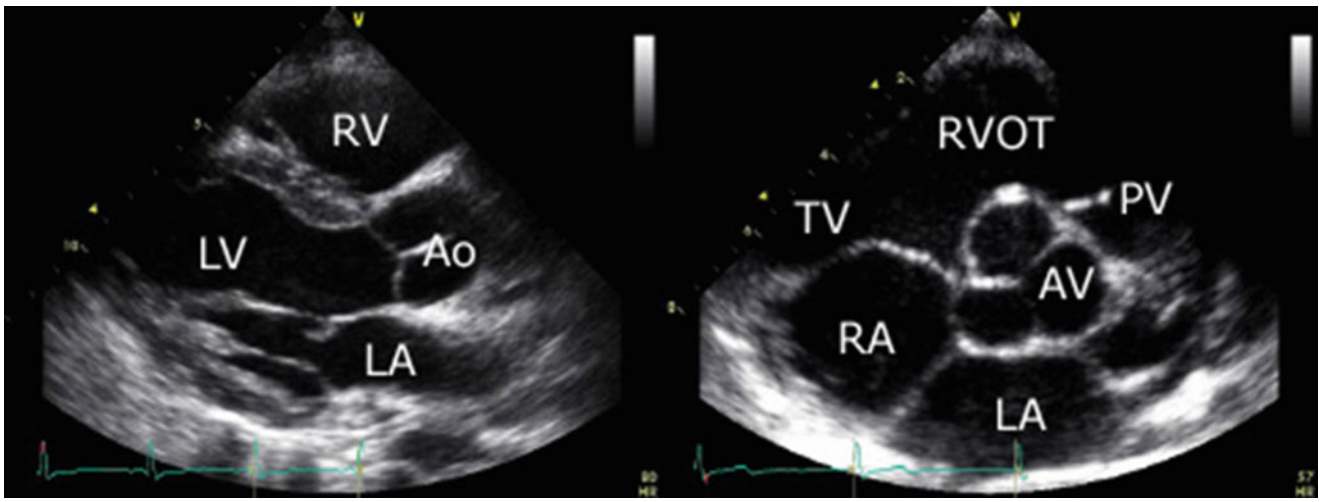

Fig. 7.26 Parasternal long-axis section through the aortic root (*left panel*) shows the closed aortic valve, while the short-axis section shows all three leaflets of the valve. *AO* aorta, *LA* left atrium, *LV* left ventricle, *RA* right atrium, *RV* right ventricle, *RVOT* right ventricular outflow tract, *PV* pulmonary valve, *TV* tricuspid valve

surgeons. Further, it is the detailed understanding of the valve features that will aid in the development and deployment of future clinical therapies, e.g., valvar repairs or replacement via either surgical or minimally invasive (transcatheter) means.

Although the anatomies of each valve type are similar, it should be noted that unique pathological changes can affect each valve resulting in differing approaches to disease assessment and treatment. Ultimately, a detailed understanding of the atrioventricular and semilunar valve anatomy will aid physicians and engineers alike in the development and deployment of future clinical therapies for the treatment of congenital and degenerative diseases affecting these valves. Furthermore, the use of common anatomical descriptions of these anatomical structures (defined as attitudinally correct anatomy) by anatomists, clinicians, and medical device designers is recommended for the successful and expedient communication of ideas and information in the modern world of medicine.

References

1. Wilcox BR, Cook AC, Anderson RH (2005) Surgical anatomy of the valves of the heart. In: Wilcox BR, Cook AC, Anderson RH (eds) Surgical anatomy of the heart. Cambridge University Press, Cambridge, pp 45–82
2. Bateman MG, Quill JL, Hill AJ et al (2013) The clinical anatomy and pathology of the human atrioventricular valves: implications for repair or replacement. J Cardiovasc Transl Res 6:155–165

3. Anderson RH, Becker AE, Allwork SP (1980) Cardiac anatomy: an integrated text and colour atlas. Gower Medical Publishing, Edinburgh/Churchill Livingstone, London
4. Bateman MG, Hill AJ, Quill JL, Iaizzo PA (2013) The clinical anatomy and pathology of the human arterial valves: implications for repair or replacement. J Cardiovasc Transl Res 6:166–175
5. Angelini A, Ho SY, Anderson RH et al (1988) A histological study of the atrioventricular junction in hearts with normal and prolapsed leaflets of the mitral valve. Br Heart J 59:712–716
6. Messer S, Moseley E, Marinescu M et al (2012) Histologic analysis of the right atrioventricular junction in the adult human heart. J Heart Valve Dis 21:368–373
7. Cook AC, Anderson RH (2002) Attitudinally correct nomenclature. Heart 87:503–506
8. Victor S, Nayak VM (1994) The tricuspid valve is bicuspid. J Heart Valve Dis 3:27–36
9. Yacoub M (1976) Anatomy of the mitral valve chordae and cusps. In: Kalmason D (ed) The mitral valve. A pluridisciplinary approach. Edward Arnold Publishers, London, pp 15–20
10. Kumar N, Kumar M, Duran CM (1995) A revised terminology for recording surgical findings of the mitral valve. J Heart Valve Dis 4:76–77
11. Ritchie J, Jimenez J, He Z et al (2006) The material properties of the native porcine mitral valve chordae tendineae: an in vitro investigation. J Biomech 39:1129–1135
12. Perloff JK, Roberts WC (1972) The mitral apparatus. Functional anatomy of mitral regurgitation. Circulation 46:227–239
13. Becker AE, de Wit APM (1979) Mitral valve apparatus. A spectrum of normality relevant to mitral prolapse. Br Heart J 42:680–689
14. Van der Bel-Kahn J, Duren DR, Becker AE (1985) Isolated mitral valve prolapse: chordal architecture as an anatomic basis in older patients. J Am Coll Cardiol 5:1335–1340
15. Gams E, Hagl S, Schad H et al (1992) Importance of the mitral apparatus for left ventricular function: an experimental approach. Eur J Cardiothorac Surg 6(Suppl 1):S17–23. Discussion S24
16. Gams E, Schad H, Heimisch W et al (1993) Importance of the left ventricular subvalvular apparatus for cardiac performance. J Heart Valve Dis 2:642–645
17. Hill AJ, Laske TG, Coles JA Jr et al (2005) In vitro studies of human hearts. Ann Thorac Surg 79:168–177
18. www.vhlab.umn.edu/atlas/index. Accessed November 20, 2014
19. Anderson RH, Devine WA, Ho SY et al (1991) The myth of the aortic annulus: the anatomy of the subaortic outflow tract. Ann Thorac Surg 52:640–646
20. Schultz CJ, Moelker A, Piazza N et al (2010) Three dimensional evaluation of the aortic annulus using multislice computer tomography: are manufacturer's guidelines for sizing percutaneous aortic valve replacement helpful? Eur Heart J 31:849–856
21. Sievers HH, Hemmer W, Beversdorf F et al (2012) The everyday used nomenclature of the aortic root components: the tower of Babel? Eur J Cardiothorac Surg 41:478–482
22. Misfeld M, Sievers HH (2007) Heart valve macro- and microstructure. Philos Trans R Soc Lond B Biol Sci 362:1421–1436
23. Marron K, Yacoub MH, Polak JM et al (1996) Innervation of human atrioventricular and arterial valves. Circulation 94:368–375
24. Filip DA, Radu A, Simionescu M (1986) Interstitial cells of the heart valves possess characteristics similar to smooth muscle cells. Circ Res 59:310–320
25. Icardo JM, Colvee E (1995) Atrioventricular valves of the mouse: III. Collagenous skeleton and myotendinous junction. Anat Rec 243:367–375
26. Icardo JM, Colvee E (1995) Atrioventricular valves of the mouse: II. Light and transmission electron microscopy. Anat Rec 241:391–400
27. Fenoglio JJ Jr, Tuan Duc P, Wit AL et al (1972) Canine mitral complex. Ultrastructure and electromechanical properties. Circ Res 31:417–430
28. Itoh A, Krishnamurthy G, Swanson JC et al (2009) Active stiffening of mitral valve leaflets in the beating heart. Am J Physiol Heart Circ Physiol 296:H1766–H1773
29. Laske TG, Shrivastav M, Iaizzo PA (2009) The cardiac conduction system. In: Iaizzo PA (ed) The handbook of cardiac anatomy, physiology, and devices, 2nd edn. Humana Press, Totowa, pp 15–21
30. Gross L, Kugel MA (1931) Topographic anatomy and histology of the valves in the human heart. Am J Pathol 7:445–473
31. Piazza N, de Jaegere P, Schulz C et al (2008) Anatomy of the aortic valvar complex and its implications for transcatheter implantation of the aortic valve. Circ Cardiovasc Interv 1:74–81
32. Carpentier A, Branchini B, Cour JC et al (1976) Congenital malformations of the mitral valve in children. Pathology and surgical treatment. J Thorac Cardiovasc Surg 72:854–866
33. Anderson RH, Razavi R, Taylor AM (2004) Cardiac anatomy revisited. J Anat 205:159–177
34. Quill JL, Hill AJ, Laske TG et al (2009) Mitral leaflet anatomy revisited. J Thorac Cardiovasc Surg 137:1077–1081
35. Barker TA, Wilson IC (2011) Surgical anatomy of the mitral and tricuspid valve. In: Bonser RS, Pagano D, Haverich A (eds) Mitral valve surgery. Springer-Verlag, London, pp 3–19
36. Delgado V, Tops LF, Schuijf JD et al (2009) Assessment of mitral valve anatomy and geometry with multislice computed tomography. JACC Cardiovasc Imaging 2:556–565
37. Kwan J, Kim G, Jeon M et al (2007) 3D geometry of a normal tricuspid annulus during systole: a comparison study with the mitral annulus using real-time 3D echocardiography. Eur J Echocardiogr 8:375–383
38. Veronesi F, Corsi C, Sugeng L et al (2009) A study of functional anatomy of aortic-mitral valve coupling using 3D matrix transesophageal echocardiography. Circ Cardiovasc Imaging 2:24–31
39. Berdajs D, Lajos P, Turina MI (2005) A new classification of the mitral papillary muscle. Med Sci Monit 11:BR18–BR21
40. Bateman MG, Russel C, Chan B et al (2010) A detailed anatomical study of the papillary muscles and chordae tendineae of the left ventricle in perfusion fixed human hearts. FASEB J. 24(Meeting Abstract Supplement):446.4
41. Sonne C, Sugeng L, Watanabe N et al (2009) Age and body surface area dependency of mitral valve and papillary apparatus parameters: assessment by real-time three-dimensional echocardiography. Eur J Echocardiogr 10:287–294
42. Lam JH, Ranganathan N, Wigle ED et al (1970) Morphology of the human mitral valve. I. Chordae tendineae: a new classification. Circulation 41:449–458
43. Kunzelman KS, Cochran RP, Verrier ED et al (1994) Anatomic basis for mitral valve modelling. J Heart Valve Dis 3:491–496
44. Ritchie J, Warnock JN, Yoganathan AP (2005) Structural characterization of the chordae tendineae in native porcine mitral valves. Ann Thorac Surg 80:189–197
45. Martinez RM, O'Leary PW, Anderson RH (2006) Anatomy and echocardiography of the normal and abnormal tricuspid valve. Cardiol Young 16(Suppl 3):4–11
46. Weinhaus AJ, Roberts KP (2009) Anatomy of the human heart. In: Iaizzo PA (ed) The handbook of cardiac anatomy, physiology, and devices, 2nd edn. Humana Press, Totowa, pp 59–85
47. Tsakiris AG, Mair DD, Seki S et al (1975) Motion of the tricuspid valve annulus in anesthetized intact dogs. Circ Res 36:43–48
48. Westaby S, Karp RB, Blackstone EH et al (1984) Adult human valve dimensions and their surgical significance. Am J Cardiol 53:552–556
49. Silver MD, Lam JH, Ranganathan N et al (1971) Morphology of the human tricuspid valve. Circulation 43:333–348
50. Seccombe JF, Cahill DR, Edwards WD (1993) Quantitative morphology of the normal human tricuspid valve: autopsy study of 24 cases. Clin Anat 6:203–212
51. Wenink AC (1977) The medial papillary complex. Br Heart J 39:1012–1018

52. Hill AJ (2009) Attitudinally correct cardiac anatomy. In: Iaizzo PA (ed) The handbook of cardiac anatomy, physiology, and devices, 2nd edn. Humana Press, Totowa, pp 15–21
53. Kunzelman KS, Grande KJ, David TE et al (1994) Aortic root and valve relationships: impact on surgical repair. J Thorac Cardiovasc Surg 107:162–170
54. Reid K (1970) The anatomy of the sinus of Valsalva. Thorax 25:79–85
55. Swanson M, Clark RE (1974) Dimensions and geometric relationships of the human aortic valve as a function of pressure. Circ Res 35:871–882
56. Brewer RJ, Deck JD, Capati B et al (1976) The dynamic aortic root: its role in aortic valve function. J Thorac Cardiovasc Surg 72:413–417
57. Thubrikar MPW, Shaner TW, Nolan SP (1981) The design of the normal aortic valve. Am J Physiol 10:H795–H801
58. Hamdan A, Guetta V, Konen E et al (2012) Deformation dynamics and mechanical properties of the aortic annulus by 4-dimensional computed tomography: insights into the functional anatomy of the aortic valve complex and implications for transcatheter aortic valve therapy. J Am Coll Cardiol 59:119–127
59. Middelhof CJFM, Becker AE (1981) Ventricular septal geometry: a spectrum with clinical relevance. In: Wenink ACG et al (eds) The ventricular septum of the heart. Martinus Nijhoff Publishers, The Hague
60. Turner K, Navartnam V (1996) The positions of coronary arterial ostia. Clin Anat 9:376–380
61. Muriago M, Sheppard MN, Ho SY et al (1997) Location of the coronary arterial orifices in the normal heart. Clin Anat 10:297–302
62. Cavalcanti JS, de Melo MN, de Vasconcelos RS (2003) Morphometric and topographic study of coronary ostia. Arq Bras Cardiol 81:359–362
63. Jo Y, Uranaka Y, Iwaki H et al (2011) Sudden cardiac arrest: associated with anomalous origin of the right coronary artery from the left main coronary artery. Tex Heart Inst J 38:539–543
64. Roynard JL, Cattan S, Artigou JY et al (1994) Anomalous course of the left anterior descending coronary artery between the aorta and pulmonary trunk: a rare cause of myocardial ischaemia at rest. Br Heart J 72:397–399
65. Sutton JP, Ho SY, Anderson RH (1995) The forgotten interleaflet triangles: a review of the surgical anatomy of the aortic valve. Ann Thorac Surg 59:419–427
66. Vollebergh FE, Becker AE (1977) Minor congenital variations of cusp size in tricuspid aortic valves: possible link with isolated aortic stenosis. Br Heart J 39:1006–1011
67. Capps SB, Elkins RC, Fronk DM (2000) Body surface area as a predictor of aortic and pulmonary valve diameter. J Thorac Cardiovasc Surg 119:975–982
68. Tops LF, Wood DA, Delgado V et al (2008) Noninvasive evaluation of the aortic root with multi-slice computed tomography: implications for transcatheter aortic valve replacement. J Am Coll Cardiol Img 1:321–330
69. Van Miegham NM, Piazza N, Anderson RH et al (2010) Anatomy of the mitral valvular complex and its implications for transcatheter interventions for mitral regurgitation. J Am Coll Cardiol 56:617–626
70. Choure AJ, Garcia MJ, Hesse B et al (2006) In vivo analysis of the anatomical relationship of coronary sinus to mitral annulus and left circumflex coronary artery using cardiac multidetector computed tomography: implications for percutaneous coronary sinus mitral annuloplasty. J Am Coll Cardiol 48:1938–1945
71. Tops LF, Van de Veire NR, Schuijf JD et al (2007) Noninvasive evaluation of coronary sinus anatomy and its relation to the mitral valve annulus: implications for percutaneous mitral annuloplasty. Circulation 115:1426–1432
72. Tawara S (1906) Das reizleitungssystem de saugetierherzens: eine anatomichhisologische studie uber das atrioventricularbundel und die Purkinjeschen faden. Verlag von Gustav Fischer, Jena
73. Asante-Korang A, O'Leary PW, Anderson RH (2006) Anatomy and echocardiography of the normal and abnormal mitral valve. Cardiol Young 16(Suppl 3):27–34
74. Otto CM (2009) Textbook of clinical echocardiography: expert consult, 4th edn. Saunders, Philadelphia
75. Baumgartner H, Hung J, Bermejo J et al (2009) Echocardiographic assessment of valve stenosis: EAE/ASE recommendations for clinical practice. J Am Soc Echocardiogr 22:1–23
76. Zoghbi WA, Enriquez-Sarano M, Foster E et al (2003) Recommendations for evaluation of the severity of native valvar regurgitation with two-dimensional and Doppler echocardiography. J Am Soc Echocardiogr 16:777–802